Alternative splicing is a developmental switch for hTERT expression

Alex Penev[1], Andrew Bazley[1], Michael Shen[2], Jef D. Boeke[2], Sharon A. Savage[3], and Agnel Sfeir[1*]

1- Skirball Institute of Biomolecular Medicine, Department of Cell Biology, NYU School of Medicine, New York, NY 10016, USA

2- Institute for Systems Genetics, Department of Biochemistry and Molecular Pharmacology, NYU School of Medicine, New York, NY 10016, USA

3- Clinical Genetics Branch, Division of Cancer Epidemiology and Genetics, National Cancer Institute, Bethesda, MD 20892, USA

Running title: Regulation of hTERT as a function of pluripotency

Keywords: hTERT, telomerase, telomeres, alternative splicing, SON

* Correspondence: Agnel Sfeir
Skirball Institute/NYU Langone Medical center
540 First Avenue
4th floor/ Lab3
New York, NY 10016
Phone: (646) 501 6742
agnel.sfeir@med.nyu.edu

High telomerase activity is restricted to the blastocyst stage of embryonic development when telomere length is reset, and is characteristic of embryonic stem cells (ESCs) and induced pluripotent stem cells (iPSCs). However, the pathways involved in telomerase regulation as a function of pluripotency remain unknown. To explore hTERT transcriptional control, we compare genome-wide interactions (4C-seq) and chromatin accessibility (ATAC-seq) between human ESCs and epithelial cells and identify several putative hTERT *cis*-regulatory elements. CRISPR/Cas9-mediated deletion of candidate elements in ESCs reduces the levels of hTERT mRNA but does not abolish telomerase expression, thus implicating post-transcriptional processes in telomerase regulation. In agreement with this hypothesis, we find an hTERT splice variant lacking exon-2 and prone to degradation, to be enriched in differentiated cells but absent from ESCs. In addition, we show that forced retention of exon-2 prevents telomerase silencing during differentiation. Lastly, we highlight a role for the splicing co-factor SON in hTERT exon-2 inclusion and identify a SON mutation in a Dyskeratosis congenita patient with short telomeres and decreased telomerase activity. Altogether, our data uncover a novel alternative splice switch that is critical for telomerase activity during development.

Telomerase counteracts telomere erosion and promotes cellular immortality. This specialized ribonucleoprotein complex is minimally composed of a reverse-transcriptase protein subunit (TERT) and an integral telomerase RNA component (TR). While the expression of telomerase RNA is ubiquitous (1, 2), TERT levels are tightly regulated (3). Human TERT (hTERT) is turned on during the blastocyst stage of embryonic development when telomere length is re-established (4), and subsequently downregulated in most somatic cells (4, 5). Similarly, hTERT becomes activated during the process of nuclear reprogramming (6) and is essential for telomere maintenance in pluripotent cells (7). Upregulation of telomerase occurs in approximately 90% of cancers, allowing tumor cells to escape crisis and proliferate indefinitely (5, 8). Somatic mutations in the hTERT promoter have been reported in a subset of cancers and shown to increase telomerase activity by creating a binding site for ETS family transcription factors (9-11). To date, the underlying mechanism that activates hTERT during development and its subsequent silencing in somatic tissues remains unknown.

The core hTERT promoter contains numerous binding sites for pluripotency and growth-related transcription factors, including Myc, Klf4, and Sp1, but expression of these different factors

is not sufficient for hTERT accumulation and telomerase activation in somatic cells (12). We therefore sought to identify *cis*-regulatory elements (REs) that could account for the difference in hTERT mRNA levels between pluripotent and somatic cells (Figure S1A). Active REs are known to directly contact the promoters they regulate and have increased chromatin accessibility, we therefore, performed Circular Chromosomal Conformation Capture (4C) and ATAC-seq in H7 human embryonic stem cells (ESC) and adult retinal pigment epithelial (ARPE) cells that are proficient for p53 and have a stable diploid karyotype. We used a 1.1 kb fragment spanning the hTERT promoter as bait and captured sequences that are in close proximity by 4C (13), using 4Cker software to analyze Illumina sequencing reads (Figure S1B-C) (14). Our analysis identified loci that contact the hTERT promoter exclusively in telomerase positive cells (H7) or in telomerase negative cells (ARPE), as well as loci that contact the TERT promoter in both cases. Notably, the majority of 4C-interactions occurred within the boundaries of the topologically associated domain (TAD) within which the hTERT locus resides (Figure 1A and Figure S1C). In parallel, we profiled genome-wide chromatin accessibility in H7 and ARPE cells using ATAC-seq (15). As expected, ATAC-seq revealed regions of open chromatin specific to each cell type, including the hTERT promoter in ESCs (Figure S1D).

By superimposing 4C interactions onto the chromatin accessibility by ATAC-seq, we identified a number of regions that displayed increased hTERT promoter interaction and open chromatin and are specific to either H7 or ARPE (Figure 1A). We identified five putative hTERT enhancers elements, termed Regulatory Elements (RE) 1-5, that displayed increased contact with hTERT promoter in H7 cells and showed an open chromatin configuration (Figure 1A). With the exception of RE4, which was reported to enhance hTERT activity in cancer cell lines, these potential enhancer elements have not been previously detected (16). Our analysis also recognized three putative hTERT transcriptional silencers elements (RE6-RE8) that show enhanced interaction with the hTERT promoter and increased chromatin accessibility in differentiated cells (Figure 1A).

To validate the putative REs, we introduced sequences corresponding to RE1-RE8 upstream of hTERT core promoter in a dual-luciferase reporter plasmid and assayed for luciferase activity in H7 and ARPE cells (Figure 1B and S1E-F). Among those tested, RE2 and RE3 significantly enhanced hTERT promoter activity in ESCs but not in somatic cells (Figure 1C and S1F). Paradoxically, the putative repressor element, RE6, also showed enhanced promoter activity in H7 cells. The latter can be explained if RE6 contained a transcription factor binding site

that is only accessible when removed from its genomic context. We combined RE2, RE3, and RE6, tandemly in the luciferase reporter and detected no additive effect on hTERT promoter activity (Figure 1C). The latter observations potentially rule out cooperativity in enhancer function during hTERT transcription. To further characterize the putative regulatory elements, we mined publicly-available ENCODE ChIP-seq data for histone modifications that distinguish active enhancers (17). Consistent with RE2 and RE3 acting as enhancers, we detected significant deposition of H3K4me1 at these loci, whereas no enrichment of H3K4me1 was evident at the RE6 locus (Figure S1G).

We next tested the enhancer function of RE2 and RE3 *in vivo* using CRISPR/Cas9 genome editing of ESCs. Our strategy entailed replacing individual enhancers with a donor sequence containing a Puromycin resistance cassette and flanked by two LoxP sites (Figure 1D). We derived independent ESC clones for each locus and confirmed homozygous targeting by genotyping PCR and Sanger sequencing (Figure 1E and data not shown). Targeted cells were then transduced with a lentiviral-encoded Cre-recombinase to excise the puromycin cassette yielding $RE2^{\Delta/\Delta}$ and $RE3^{\Delta/\Delta}$ cells (Figure 1E). We performed quantitative RT-PCR and observed two to four-fold reduction in hTERT mRNA levels in enhancer-deleted cells, confirming enhancer activity for both RE2 and RE3 (Figure 1F). In addition, we generated double-knockout $RE2^{\Delta/\Delta}RE3^{\Delta/\Delta}$ ESCs and observed that dual targeting of both enhancers did not lead to further reduction in hTERT transcript when compared to $RE2^{\Delta/\Delta}$ cells (Figure 1F and Figure S1H). These results provided further support that the two enhancers do not act cooperatively during hTERT transcriptional activation. Despite the noted reduction in hTERT mRNA levels, Telomere Repeat Addition Processivity (TRAP) assay revealed that cells lacking RE2 and RE3 had similar telomerase activity as non-targeted cells (18) (Figure 1G). Given that the reverse transcriptase encoded by hTERT is not rate limiting for telomerase activity in human ESCs (11), a four-fold reduction in hTERT mRNA is not expected to impact overall telomerase activity in H7 cells. In summary, our analysis identified RE2 and RE3 as novel enhancer elements that modulate hTERT mRNA levels in ESCs *vs.* differentiated cells. Nonetheless, the maximal reduction for telomerase transcripts in enhancer-deleted cells was significantly less than the observed 100-fold difference in hTERT expression between pluripotent and differentiated cells (Figure S1A). While we cannot rule out that additional distant enhancer elements might further regulate hTERT transcription, it is also possible that transcriptional regulation alone does not account for the strong induction of telomerase in ESCs and its subsequent repression in differentiated cells. To test this idea, we transduced wildtype fibroblasts with Vp64-dCas9 fusion protein and two guide RNAs

complementary to the hTERT promoter (19). We then performed RT-qPCR and observed minimal hTERT activation in Vp64-dCas9 expressing fibroblasts relative to ESCs (Figure S1I). Based on these results, we concluded that recruitment of a robust transcriptional activator to the hTERT promoter in differentiated fibroblasts led to only mild accumulation of telomerase mRNA.

We next sought to explore the impact of post-transcriptional processing on the abundance and stability of hTERT mRNA in ESCs. Specifically, we focused on alternative splicing of pre-mRNA as a regulatory pathway that has been previously shown to control developmentally-regulated genes and pluripotency-associated factors (20-25). Many hTERT alternative splice variants have been detected in different cell types, including α/β variants that modulate telomerase activity in cancer cells (26-28). We analyzed the full spectrum of telomerase splice variants in H7 and ARPE cells using RNA Capture-seq that combines tiling arrays of biotinylated oligos with RNA-seq and therefore, enhances the sequencing coverage for low abundance transcripts such as hTERT. hTERT Capture-seq identified notable reads spanning exon-1 and exon-3, indicative of hTERT transcripts lacking exon-2 (hTERT-ΔEx2), that were abundant in differentiated cells but not ESCs (Figure 2A-B). These results are consistent with a previous meta-analysis, in which transcripts lacking exon-2 were consistently and widely expressed in many human cell types except ESCs (29).

To corroborate the results of the RNA Capture-Seq, we designed a junction-specific PCR strategy in which cDNA was first generated with a gene-specific primer in hTERT exon-4 and subjected to exon-spanning quantitative PCR to determine the ratio of hTERT-ΔEx2 relative to full-length hTERT mRNA (Figure 2B-C). Our analysis revealed that hTERT-ΔEx2 was 4 times more abundant than full-length transcript in cells lacking telomerase activity, including epithelial cells (ARPE) and fibroblasts (BJ). In contrast, ESCs and iPSCs derived from BJ fibroblasts displayed diminished levels of hTERT-ΔEx2. In conclusion, junction-PCR analysis further confirmed a strong correlation between exon-2 skipping and the absence of telomerase activity in differentiated cells (Figure 2D). Importantly, we detected the same correlation between telomerase activity and exon-2 alternative splicing in RNA samples obtained from human tissues, including brain (telomerase negative) and testis (telomerase positive) (Figure S2A).

Exclusion of hTERT exon-2 is predicted to generate tandem premature termination codons in exon-3 that would act as signal for mRNA decay (30) (Figure 2B). We examined the effect of inhibiting the RNA decay machinery on the abundance of hTERT transcripts. To that end,

we performed junction-specific RT-qPCR following the transient depletion of nonsense-mediated decay factor, UPF1. Our results revealed increased accumulation of hTERT-ΔEx2 transcripts in HeLa cells lacking UPF1 (Figure S2B). We obtained similar results upon treatment of cells with small molecule inhibitors for the RNA decay machinery (Figure S2C), suggesting that exon-2 skipping yields transcripts that are susceptible to degradation. In a complementary approach, we transfected HeLa cells with splice-blocking anti-sense morpholinos (ASOs) that specifically prevented the inclusion of exon-2. This then led to increased accumulation of hTERT-ΔEx2 variant mRNA and a concomitant reduction in transcripts containing exon-2 (Figure S2D-E). In agreement with exon-2 exclusion compromising telomerase function, we noted a significant reduction in TRAP activity in cells treated with exon-2 ASO relative to control cells (Figure S2F-G). Taken together, our results indicate that selective transcripts lacking exon-2 trigger the nonsense-mediated decay machinery to degrade hTERT mRNA and compromise telomerase function.

So far, our data uncovered a strong correlation between exon-2 inclusion and the accumulation of hTERT transcripts. We next tested the impact of forced exon-2 retention on telomerase silencing during differentiation by targeting the first intron of hTERT in human ESCs with CRISPR/Cas9 (Figure 3A). In effect, deletion of hTERT intron-1 results in a constitutive fusion between exon-1 and exon-2 and thus prohibits the alternative splicing event that results in exon-2 exclusion. We performed two separate rounds of gene-editing and isolated a total of six independent hTERT$^{\Delta in1/\Delta in1}$ clones that we validated using genotyping PCR and Sanger sequencing (Figure 3B and S3A). hTERT$^{\Delta in1/\Delta in1}$ ESCs maintained proper morphology and expressed appropriate cell surface markers (Figure S3B) (6). Furthermore, telomerase activity in hTERT$^{\Delta in1/\Delta in1}$ ESCs was similar to that of hTERT$^{+/+}$ cells (Figure S3D). We then differentiated hTERT$^{\Delta in1/\Delta in1}$ ESCs into fibroblasts and confirmed downregulation of key pluripotency genes and a concomitant upregulation of fibroblast-specific genes (Figure S3B-C). As expected, we observed complete repression of hTERT upon differentiation of hTERT$^{+/+}$ ESCs (Figure 3C) (4, 31). In contrast, hTERT$^{\Delta in1/\Delta in1}$ fibroblasts retained significant hTERT mRNA levels by quantitative RT-PCR (Figure 3C). To further corroborate the failure of hTERT silencing in differentiated hTERT$^{\Delta in1/\Delta in1}$ cells, we quantified hTERT mRNA directly using custom NanoString^{TM} probes and noted the retention of sequences corresponding to several exons (Figure 3D). Additionally, we examined hTERT mRNA abundance and localization using single-molecule RNA-FISH probes (sm-FISH) (32) and confirmed its accumulation in hTERT$^{\Delta in1/\Delta in1}$ but not hTERT$^{+/+}$ fibroblasts (Figure S3E). sm-FISH revealed that hTERT transcripts in hTERT$^{\Delta in1/\Delta in1}$ cells are capable of being

exported from the nucleus, albeit not as efficiently as pre-spliced hTERT cDNA. Lastly, we showed that the abrogation of hTERT silencing was not limited to hTERT$^{\Delta in1/\Delta in1}$ fibroblasts but was also evident when ESCs were differentiated into hepatocyte-like cells *in vitro* (Figure S4A-B) (33).

To rule out that intron-1 contained a cis-regulatory element that enforced hTERT silencing in differentiated cells, we introduced the corresponding sequence into the dual-luciferase reporter assay and detected no difference in hTERT promoter activity (Figure S4C). Additionally, we generated clonally-derived ESCs in which hTERT intron-1 was replaced with scrambled intronic sequence that retained the splice junctions (Figure S4D), and found that hTERT mRNA levels were similar to non-targeted ESCs (Figure S4E). In conclusion, our results demonstrated that forced retention of hTERT exon-2 prevents telomerase silencing in differentiated cells. We then examined telomerase enzymatic function and observed increased TRAP activity in hTERT$^{\Delta in1/\Delta in1}$ fibroblasts relative to differentiated hTERT$^{+/+}$ cells (Figure 3E and Figure S4F). These results further support that exclusion of exon-2 is a key step during telomerase silencing upon differentiation. It is worth noting that although hTERT$^{\Delta in1/\ \Delta in1}$ fibroblasts retained significant levels of hTERT mRNA, telomerase activity in the targeted fibroblasts was significantly lower than ESCs. It is established that modification of pre-mRNA influences post-transcriptional processes (34, 35), including mRNA modification, nuclear export, and translation efficiency that could be compromised in differentiated cells.

Having explored hTERT regulation by transcriptional activation and alternative splicing separately, we next sought to investigate the interplay between the two processes during telomerase activation. To that end, we exploited the dCas9-Vp64 transactivation system to increase hTERT promoter activity in hTERT$^{\Delta in1/\ \Delta in1}$ and hTERT$^{+/+}$ fibroblasts, independently (Figure 3F and S4G). Analysis of hTERT mRNA by quantitative RT-qPCR revealed that while transcriptional activation has\d a minimal impact in wildtype cells, a synergistic effect on hTERT mRNA accumulation was observed when Vp64-dCas9 was recruited to the hTERT promoter in hTERT$^{\Delta in1/\ \Delta in1}$ cells (Figure 3F). In summary, we conclude that transcriptional activation is not sufficient to mount robust hTERT levels in differentiated cells. Instead, our data is consistent with promoter activation being coupled to exon-2 retention by alternative splicing to allow the accumulation of hTERT mRNA.

In order to provide insight into the mechanism underlying alternative splicing of hTERT exon-2 and identify factors that influence exon choice, we carried out a small-scale RNAi-screen using luciferase-reporter genes. We generated two synthetic doxycycline-inducible “minigenes” comprising hTERT exons 1 to 3 and the spanning introns (Figure 4A). In the first minigene, Firefly luciferase was in-frame with the hTERT ORF containing exon-2 and therefore expressed only when the second exon was incorporated into the mRNA. Conversely, in the second minigene, Nano-luciferase was placed downstream of hTERT-ΔEx2 reading frame and was specifically expressed upon exclusion of exon-2. Both minigenes were assembled in yeast by homologous recombination (36) and included FRT sites to facilitate their integration into T-REx™-HeLa cells (Figure S5A-B). HeLa cells express hTERT-ΔEx2 and full-length transcripts at similar levels and were therefore suitable to investigate factors that regulate telomerase alternative splicing (Figure S5C). We co-transfected HeLa-FRT cells with minigenes I & II and established a clonally derived cell line with heterozygous integration of both minigenes at the same locus. In order to calculate the ratio of hTERT-ΔEx2 transcripts relative to full-length mRNA, we measured Firefly and Nano luciferase activity 48 hours after doxycycline treatment (Figure S5D). Upon validating the minigene reporter line, we assembled an siRNA mini-library targeting 442 genes annotated as RNA-binding proteins and splicing factors (Supp. Table 3) (37) and performed a small-scale RNAi screen. We monitored dual luciferase activity and found that knockdown of 77 genes significantly altered Nano:Firefly ratio ($p<0.05$) (Figure 4B). Top siRNA hits that enhanced inclusion of exon-2 included RBM14, a paraspeckle protein involved in nuclear RNA sequestration (38) and Mbnl1, a splicing regulator that represses pluripotency-associated exon inclusion (23). On the other hand, candidates that increased the ratio of Nano:Firefly luciferase and therefore, promoted the exclusion of hTERT exon-2 comprised multiple SF3A/B family members and the testis specific factor, BrdT.

The strongest hit from our small-scale RNAi screen was the nuclear speckle protein and alternative splicing co-factor, SON. Knockdown of SON resulted in a significant increase in the ratio of Nano:Firefly luciferase, indicative of strong exon-2 exclusion. SON is enriched in ESCs and some cancer cells and has been shown to be required for splicing of pluripotency genes by facilitating the inclusion of exons with weak consensus splicing sites (39) (40). Given that long-term inhibition of SON was previously shown to impair pluripotency (39), we transiently depleted the gene in H7 and HeLa cells using siRNA (Figure S5E). As a control, we showed that expression of pluripotency genes was maintained 48 hours post-SON knockdown (Figure S5G). Junction RT-PCR revealed that SON inhibition led to a significant increase in hTERT-ΔEx2 and a concomitant

decrease in full-length telomerase transcripts (Figure 4C and Figure S5F). In agreement with exon-2 skipping leading to compromised hTERT mRNA stability, SON depletion resulted in a significant decrease in TRAP activity in ESCs as well as HeLa cells (Figure 4D-E and S5H-I). In conclusion, our results identify SON as a key regulator of hTERT exon-2 splicing and highlights its role in controlling telomerase activity.

Mutations in SON have been identified in a number of patients diagnosed with intellectual-disability and developmental disorders (41), and one proband was also diagnosed with dyskeratosis congenita (DC), an inherited bone marrow failure syndrome (IBMFS) due to very short telomeres as a result of pathogenic germline variants in the telomerase pathway. DC patients are characterized by the diagnostic triad of nail dystrophy, abnormal skin pigmentation, oral leukoplakia, as well as high rates of bone marrow failure, cancer, pulmonary fibrosis and other complications (42). We identified a female patient (NCI-550-1) with the DC mucocutaneous triad, history of leukopenia, and an additional clinical diagnosis of Zhu-Tokita-Takenouchi-Kim (ZTTK) syndrome (41); an intellectual-disability syndrome associated with cerebral malformations, epilepsy, vision abnormalities, and dysmorphology. The patient is heterozygous for a premature termination allele of the SON gene SON Q96X (chr21:34,921,823, c.286C>T) (Figure 4F). We measured telomere length in granulocytes and lymphocytes using flow cytometry in-situ hybridization (Flow-FISH) and noted very short telomeres (≤1st percentile) in the proband compared to the healthy population (Figure S6). Furthermore, we performed TRAP assay on lysates obtained from peripheral blood mononuclear cells (PBMCs) obtained from the proband and noted substantially reduced telomerase activity relative to a healthy subject (Figure 4G-H). Collectively, our results reveal that SON alternations compromises telomerase activity leading to telomere shortening that might contribute to disease manifestation.

It is well-established that high telomerase levels in the early stages of development resets telomere reserves which is critical for tissue renewal, prevention of degenerative disorders, and possibly setting longevity. Yet, over 30 years since the discovery of telomerase, the fundamental question of how hTERT becomes activated in the inner cell mass and subsequently repressed in differentiated cells remains elusive. Based on our data, we propose a model where hTERT is dually regulated by transcriptional as well as post-transcriptional processes. We show that transcriptional regulation is driven by *cis*-regulatory elements that control hTERT promoter activity. Importantly, our findings indicate that alternative splicing an molecular gatekeeper for hTERT regulation as a function of pluripotency. Specifically, we highlight a previously

unanticipated alternative-splice switch centered around exon-2 that ensures the accumulation of full-length hTERT in pluripotent cells. Exclusion of hTERT exon-2 serves to completely repress telomerase activity in somatic cells and enforces the tumor suppressor function of telomere shortening. This is supported by the identification of TERT alternative splice variants in additional species, as evolutionarily distant as Planarians (26, 43, 44). Our study also implicates SON in the regulation of this key alternative splicing switch and we link SON mutations with telomere shortening in a DC patient. At this stage, we cannot exclude that SON mutations impair telomerase activity indirectly by altering levels of other cellular RNAs. However, given the direct role for SON in regulating hTERT exon choice (Figure 4B-C), we favor the scenario where disruption of SON directly impacts telomerase biogenesis. In addition, our results underscore a potential therapeutic benefit for targeting hTERT alternative splicing to block telomerase in cancer cells. Alternatively, enhanced inclusion of hTERT exon-2 might boost telomerase activity in syndromes associated with short telomeres and in regenerative medicine therapies.

Acknowledgements: We thank Marion Pouillard for her assistance in the early stages of this project. We acknowledge Eros-Lazzerini Denchi and members of the Sfeir lab for comments on the manuscript. We thank Luis Batista for sharing methods for hepatocyte differentiation. Lei Bu, Jerry Shay, and Maria Barna are thanked for reagents. We also thank Ashley S. Thompson for assistance with gene and variant curation. We acknowledge the genome technology core (GTC), high throughput biology (HTB) core, Michael Cammer and the microscopy core at NYU School of medicine. This work was supported in part by a grant from the Irma T. Hirschl foundation to A.S. an NIH fellowship to A.P, and NIH grant RM1HG009491 to J.D.B. The authors would like to dedicate this study to the memory of Woodring E. Wright.

Author Contributions: A.S. and A.P. conceived the experimental design. All experiments were performed by A.P. A.B. assisted with RNAi screen. M.S. in the lab of J.D.B. helped generate the minigene reporters. S.A.S. evaluated clinical data on the patient with the identified SON mutation. A.S. and A.P. wrote the manuscript. All authors discussed the results and commented on the manuscript.

Author information: Agnel Sfeir is a co-founder, consultant, and shareholder in Repare Therapeutics. J.D.B. is a founder and director of the following: Neochromosome, Inc., the Center of Excellence for Engineering Biology, and CDI Labs, Inc. and serves on the Scientific Advisory Board of the following: Sangamo, Inc., Modern Meadow, Inc., and Sample6, Inc.

Correspondence and requests for materials should be addressed to A.S. agnel.sfeir@med.nyu.edu.

Figure Legends:

Figure. 1. Identification of novel cis-regulatory elements (REs) that modulate hTERT expression as a function of pluripotency. A) Top: Refseq of annotated genes on chr5, depicting candidate RE elements within the TAD boundary surrounding the hTERT locus (grey box). Bottom: Overlay of data obtained from ATAC-seq and 4C-seq analysis to identify candidate hTERT REs. Candidate enhancers (left, RE1-RE5) preferentially interact with hTERT promoter and display open chromatin in embryonic stem cells (ESCs). Silencer elements (right, RE6-RE8) interact with hTERT promoter in differentiated cells. 4Cker software was used to determine interaction score (line graphs) and was aligned to ATAC-seq results from three independent replicates. B) Schematic of the dual luciferase reporter used to interrogate the function of individual REs. hTERT core promoter is composed of 500bp sequence upstream of transcription start site (TSS) as well as 100bp downstream sequence encompassing hTERT start codon. Individual REs were cloned upstream of hTERT promoter. Expression of Renilla luciferase driven by a constitutive promoter for normalization. A strong hairpin is positioned downstream of the Renilla gene to prevent transcriptional read-through. C) Bar graph represents the ratio of Firefly to Renilla luciferase in ESCs expressing the reporter plasmid with the indicated RE (n=3, *: $p<0.05$, **: $p<0.01$, ***: $p<0.001$). D) Schematic of CRISPR/Cas mediated gene editing of RE2 and RE3 in human ESCs. Cells were co-transfected with two sgRNA that cut on either side of the 500bp locus and a double-stranded (ds) DNA donor containing Puromycin resistance cassette. Following targeting, excision of Puromycin cassette was carried out using lentiviral Cre recombinase. Arrows indicate primers used for genotyping. E) Genotyping PCR on cells with the indicated genotype and Cre-treatment using primers highlighted in (D). PCR products (RE2/RE3): wild type, 560/700bp; targeted, 1500/1700bp and null alleles, 250/300bp F) Quantitative RT-PCR for hTERT mRNA in cells with the indicated genotype following treatment with Cre recombinase. (n=3, $RE3^{\Delta/\Delta}$: $p<0.01$, $RE2^{\Delta/\Delta}$ and DKO: $p<0.0001$). G) Telomere Repeat Addition Processivity (TRAP) assay to measure telomerase holoenzyme activity in clonally derived ESCs lacking the indicated RE. HI=heat inactivated

Figure. 2. **Inclusion of exon-2 correlates with the abundance of telomerase mRNA**. A) Sashimi plot representing RNA Capture-Seq for hTERT locus in H7 ESCs and ARPE cells. Reads from exons are depicted as pileups and exon-exon junctions denoted with arcs. Asterisks indicate ΔEx2 splice variant transcripts detected in differentiated cells. B) Schematic of full-length and hTERT-ΔEx2 transcripts, demonstrating the position of the premature termination codons (PTC,

asterisks) generated upon exon-2 skipping. Two tandem PTC's would likely target ΔEx2 transcript for degradation by nonsense-mediated decay (NMD). C) Schematic illustration of junction-spanning PCR strategy used to assay hTERT ΔEx2 abundance by quantitative RT-PCR. RNA was reverse-transcribed using an hTERT gene-specific primer (GSP) and cDNA was purified and equalized between samples prior to PCR amplification with the indicated primers. D) Quantification of the ratio of hTERT ΔEx2 relative to full-length as determined by qRT-PCR in mortal cell lines (ARPE & BJ), ARPE and BJ cell lines immortalized with hTERT cDNA, iPSCs derived from BJ cells, and human ESCs (n=3, $p<0.0001$).

Figure 3. Forced retention of exon-2 abolishes silencing of hTERT upon differentiation. A) Schematic illustration of intron 1 deletion by CRISPR/Cas9 gene editing and the predicted splicing pattern. Cells were co-transfected with two sgRNA that cleave within hTERT intron-1 and a 200bp single-stranded (ss) DNA donor containing 100bp sequence from exon-1 and exon-2 directly concatenated. B) Genotyping PCR from cells with the indicated genotype. PCR products: wild type, 584bp; Δintron1, 480bp C) Quantitative RT-PCR for hTERT mRNA in cells with the indicated genotype. hTERT expression is silenced in fibroblasts derived from wildtype ESC clones, whereas hTERT levels remain elevated upon differentiation of $hTERT^{\Delta in1/\Delta in1}$ ESCs. Values are normalized to $hTERT^{+/+}$ H7 ESC (n=3, **: $p<0.01$, ***: $p<0.001$, ****: $p<0.0001$). D) Absolute quantification of multiple hTERT exon-exon junctions using direct Nanostring quantification of RNA confirms increased hTERT transcripts in fibroblasts derived from $hTERT^{\Delta in1/\Delta in1}$ ESCs. Data normalized to $hTERT^{+/+}$ ESCs (n=3, $p<0.001$). E) TRAP assay for telomerase activity in cells with the indicated genotype shows that $hTERT^{\Delta in1/\ \Delta in1}$ fibroblasts retain telomerase activity compared to wildtype control cells. F) RT-qPCR for hTERT mRNA in differentiated fibroblasts in the context of Vp64-Cas9 transcriptional activation of hTERT promoter. Two $hTERT^{+/+}$ and $hTERT^{\Delta in1/\Delta in1}$ clones were transduced with lentivirus encoding Vp64-dCas9 transactivation protein and 2 guide RNAs complementary to hTERT promoter. Following FACS selection of Vp64-dCas9 expressing cells, RT-qPCR was performed on non-transduced parental clonal lines and Vp64-dCas9 expressing cells. Values normalized to H7 cells (n=3, $p<0.01$).

Figure 4. **SON is a key regulator of hTERT alternative splicing.** A) Schematic of minigenes designed to measure the efficiency of hTERT mRNA splicing using Nano- and Firefly luciferase activity as a readout. Retention of exon-2 leads to expression of Firefly luciferase, but not Nano luciferase. Conversely, exclusion of exon 2 leads to a (-1) frameshift in exon-3 prompting the expression of Nano-luciferase while shifting Firefly luciferase out-of-frame. B) The minigenes

were integrated into HeLa cells and a small-scale RNAi screen using a curated list of splicing factors and RNA-binding proteins was performed. Graph depicts the average ratio of Nano/Firefly luciferase of 3 biological replicates for 442 genes. Data presented as a log-ratio, colors highlight genes with p-value <0.05. Genes highlighted in green are putative positive regulators of hTERT, and genes in blue are negative regulators of hTERT expression. C) Quantification of the abundance of hTERT exon1-2 and exon1-3 splice-junctions in ESCs following knockdown of SON. (n=4, p<0.001). D) Representative TRAP assay to detect telomerase activity in ESCs, 48 hours after SON depletion with siRNA. E) Quantification of the TRAP assay as in D. F) Pedigree highlighting the proband, a female child of unaffected parents, carrying a de novo SON Q96X heterozygous mutation (Q96X) affected with ZTTK and DC. G) Representative TRAP assay for telomerase activity in PBMC from a healthy donor (WT) and the proband (SON). PBMC from a PARN patient was used as a control H) Quantification of the TRAP assay in (G) (p<0.01). WT – TA 4646 0523. PARN – NCI-382-1 – TA 2812 0860 mutation p.N7H (c.19A>C) and deletion chr16:14,037,911 - 15,319,123 (patient published in (45)). SON – NCI-550-1– TA 5330 0534 mutation c.286C>T exon 3 p.Q96X

Figure 1

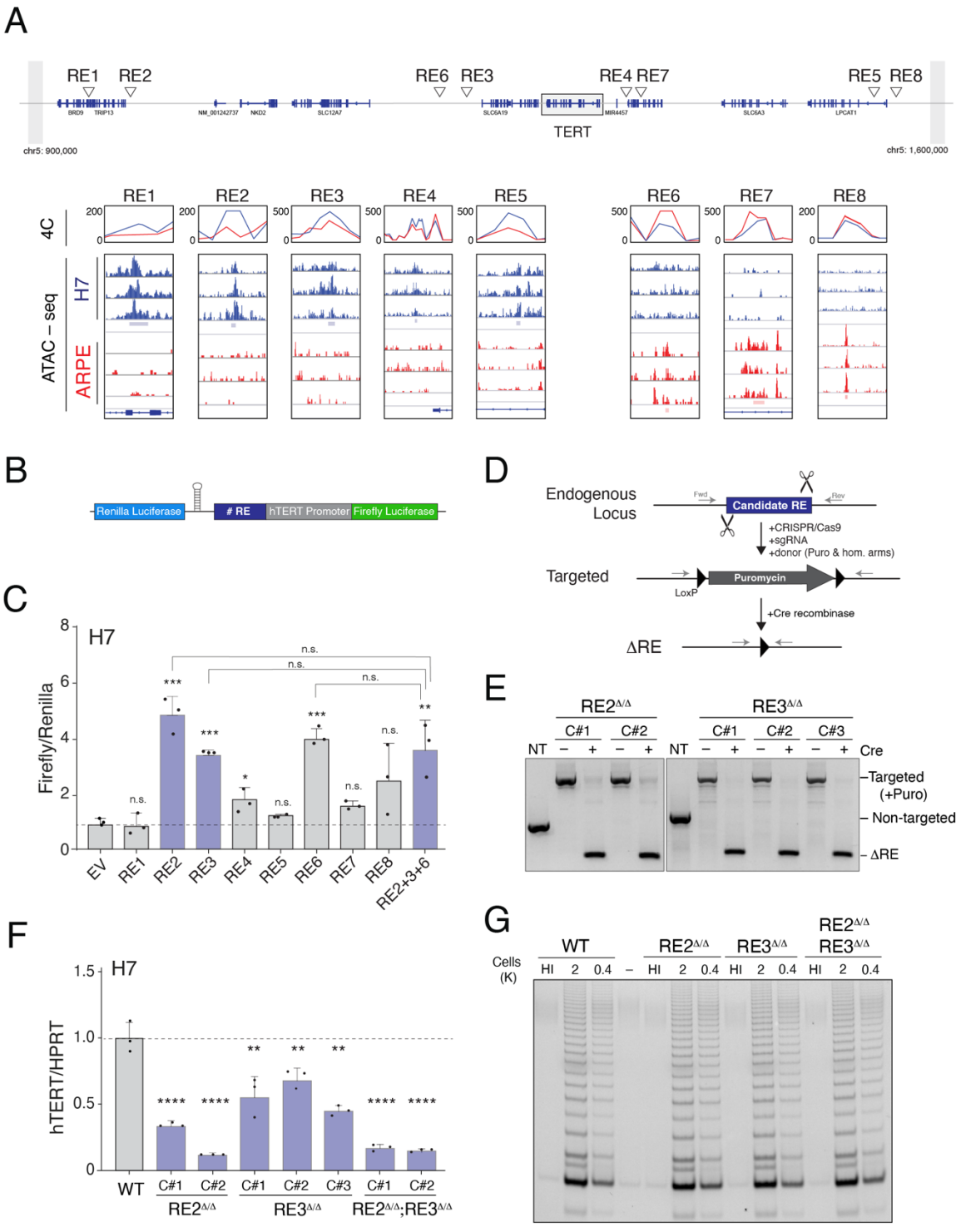

Figure 2

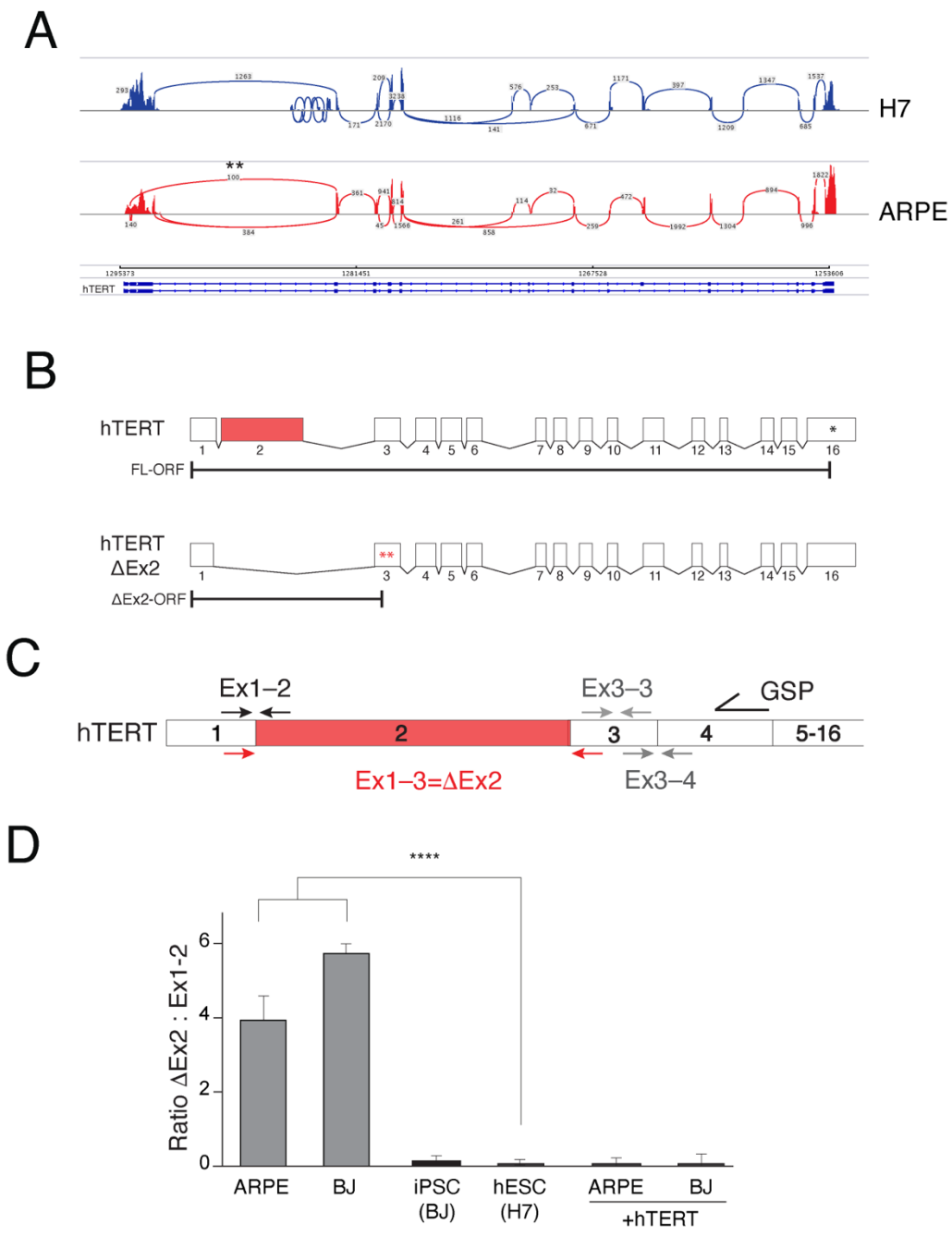

Figure 3

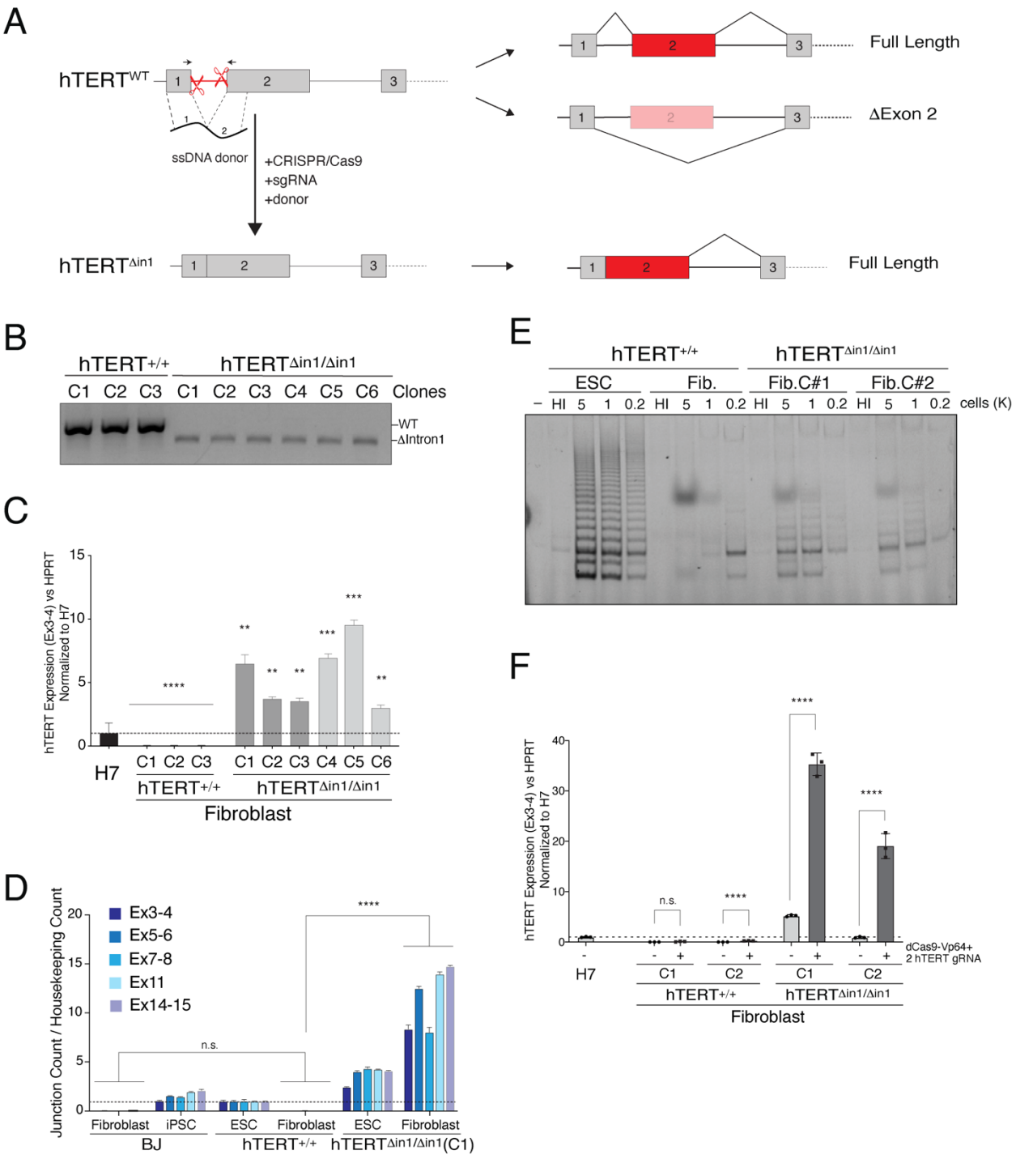

Figure 4

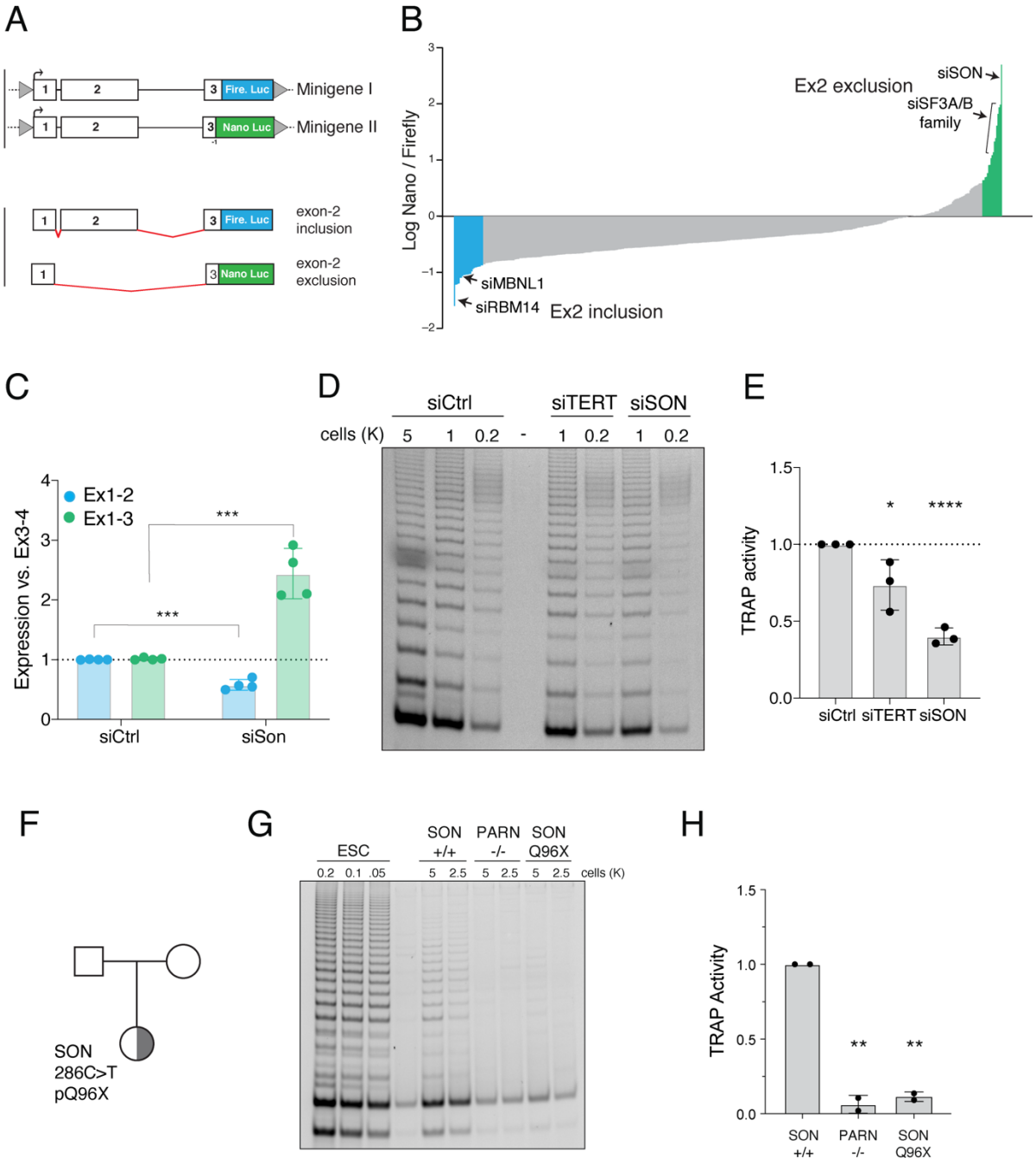

METHODS

Cell culture procedures and treatments

ARPE-19 cells (ATCC© CRL-2302™), HeLa (ATCC® CCL-2), T-REx™-HeLa (Invitrogen™) and BJ cells (ATCC® CRL-2522™) in Dulbecco's Modified Eagle Medium (DMEM, Corning™) supplemented with 10% fetal bovine serum (FBS, Gibco™), 2 mM L-glutamine (Gibco™), 100 U/ml Penicillin-Streptomycin (Gibco™), and 0.1 mM MEM non-essential amino acids (Gibco™). ARPE-19 and BJ cell lines were immortalized with hTERT and cultured in the same media conditions. Cells were passaged every 48-72 hours and maintained mycoplasma free by using Plasmocin™ (Invivogen) *per* manufacturer indication. *H7* human embryonic stem cells were a kind gift from Lei Bu and cultured in mTeSR™ Plus (STEMCELL™) media supplemented with 100 U/ml Penicillin-Streptomycin (Gibco). ESCs were passaged every 2-3 days using 500 µM EDTA in PBS and recovered for one day in Y-27632 2HCl (5-10 µM, SelleckChem®). *293T* cells used for lentiviral packaging were cultured in DMEM supplemented with 10% bovine calf serum (BCS, Gemini), 2 mM L-glutamine (Gibco™), 100 U/ml Penicillin-Streptomycin (Gibco™), 0.1 mM MEM non-essential amino acids (Gibco™). hTERT minigene expression was induced with 2 µM doxycycline (Sigma-Aldrich®) for 48 hours following siRNA tranfections.

iPSC reprogramming of BJ fibroblasts was performed using CytoTune™- iPS Sendai Reprogramming kit (ThermoFisher) as per manufacturer instructions. Fibroblast differentiation from hESCs was performed in differentiation media containing 15% fetal bovine serum (FBS, Gibco™), 2 mM L-glutamine (Gibco™), 100 U/ml Penicillin-Streptomycin (Gibco™), and 0.1 mM MEM non-essential amino acids (Gibco™). Media was changed without passaging every two days for 21 days when fibroblast differentiation was complete. Cells were subsequently passaged every 4-5 days. Hepatocyte differentiation was performed as described in Mallanna et al. (33) with media changes every 2 days. Briefly, ESCs were plated in Geltrex™ (Gibco) coated 6-well plates and treated with RPMI 1640 (Corning) media containing 2% B27 supplement (w/o insulin, Gibco), and additional recombinant factors including Activin A (100ng/ml, Thermo), BMP4 (10ng/ml, Thermo), FGF2 (20ng/ml, Thermo) for two days. Day 3-5 media contained only Activin A in B27-RPMI 1640 media. Day 6-10 media contained 2% B27 supplement with insulin (Gibco) and BMP4 and FGF2 at previous concentrations. Days 11-15 media contained recombinant HGF (20ng/ml, Thermo) in B27+insulin RPMI 1640 media. Days 16-24 media contained recombinant Oncostatin M (20ng/ml, Thermo) in HCM media lacking EGF (Lonza).

For cell treatments, the following compounds were used: 5-fluoro-uracil (50 μM, Sigma-Aldrich®), Isoginkgetin (20 μM, Cayman Chemicals®).

The patient was a participant the IRB-approved longitudinal cohort study titled Etiologic Investigation of Cancer Susceptibility in Inherited Bone Marrow Failure Syndromes (NCT-00027274). Informed consent was signed by her parents and data were collected through questionnaires and medical record review (46).

4C and ATAC-seq genome-wide sequencing and bioinformatic analysis

Library preparation for Circular Chromosome Conformation Capture (4C) was performed as described in van de Werken et al 2012 (13) with the exception of initial fixation and lysis procedure, which was adapted from Miele et al 2009 (47). $1x10^7$ ARPE or H7 ESCs were dissociated and resuspended in 5ml PBS containing 10% BCS. Cells were crosslinked by adding 5ml of 4% formaldehyde in PBS and incubating at room temperature (RT) for 10 minutes with gentle rocking. Reaction was quenched by adding 2.5ml 2.5M glycine, mixing well and incubating at RT for 5 minutes, then on ice for 15 minutes. Cells were pelleted at 800xg for 10 minutes, resuspended in 1ml of cold Lysis Buffer 1 (10mM Tris pH 8.0, 10mM NaCl, 0.2% IGE-PAL, Protease inhibitor (Roche)) and incubated on ice for 15 minutes. Cells were then dounce-homogenized on ice with a B-type pestle twice for 15 minutes with a minute rest on ice in between. Sample was pelleted at 2500xg for 5 minutes and the pellet was washed with 1x Cutsmart buffer (NEB) and pelleted again. Samples were further processed as described in van de Werken 2012 (13) using DpnII primary digestion and Csp6I secondary digestion. Sequencing library was prepared as described using Expand Long Template polymerase (Roche) and Illumina adaptor sequence-containing primers unique to the hTERT fragend listed in Supplementary Table 1. Sequencing was performed by the NYU Genome Technology Core on Illumina HiSeq 4000 sequencer. Sequencing data was analyzed using the 4Cker software package described in (14) using the recommended parameters.

ATAC-seq was performed on $5x10^5$ ARPE and H7 cells in triplicate as described in Buenrostro et al. 2015 (15). Sequencing of libraries was performed by NYU Genome Technology on Illumina HiSeq 2500 sequencer. Alignment was performed as in Buenrostro et al. 2013 (48) to the hg19 human reference genome and peak calling was done using macs2 using parameters described in Corces et al. 2017 (49). IGV was used to visualize sequencing data tracks and bedtools was used for find regions of overlap between ATAC-seq and 4C data.

Dual-Luciferase assay for hTERT promoter activity

Dual luciferase reporter plasmid pRF-HCV was a kind gift from Maria Barna (50). HCV promoter was replaced with hTERT core promoter sequence amplified from ESC genomic DNA and cloned into pRF using NcoI restriction enzyme sites. Candidate sequences were similarly amplified from genomic DNA and cloned into BbvCI restriction enzyme site upstream of hTERT promoter. Plasmid DNA was purified using Plasmid Plus Midi Kit (Qiagen) or NucleoBond Xtra Midi Kit (Machery Nagel). Reporter plasmid was introduced to H7 and ARPE cells via transient transfection. Cells were lysed 48 hours after transfection and assayed for luciferase activity using the Dual-Luciferase Reporter Assay System (Promega) according to the manufacturer's instructions using a Flexstation 3 Multi-mode Microplate Reader (Molecular Devices). Each sample was assayed in triplicate.

Real-Time RT-qPCR

Total RNA was purified with RNAeasy Mini Kit (Qiagen) or NucleoSpin® RNA Clean-up (Macherey-Nagel) following manufacturer instructions. Genomic DNA was eliminated by on-column digestion with DNaseI. A total of 1 µg of RNA was reverse-transcribed using iScript Reverse Transcription Supermix (Biorad) and qPCR (45 cycles) was performed on a Roche LightCycler480. Reactions were run in triplicates with ssoAdvanced SYBR green Supermix (Biorad) in a total volume of 10µl with standard cycling conditions. Relative gene expression was normalized using HPRT or TBP as housekeeping genes and all calculations were performed in Excel. A list of primers is available in Suppl. Table 1.

RT-qPCR for hTERT exon-exon junctions

Total RNA was purified with RNAeasy Mini Kit (Qiagen) or NucleoSpin® RNA Clean-up (Macherey-Nagel) following manufacturer instructions. Genomic DNA was eliminated by on-column digestion with DNaseI. A total of 10 µg of RNA was reverse-transcribed using Superscript IV Reverse-Transcription kit (Invitrogen) using an hTERT specific probe in exon-4 (CCTGACCTCTGCTTCCGACAG). Primer was annealed to hTERT RNA at 65C for 5 minutes and then incubated at 0C for 5 minutes before addition of other kit reagents. Reaction was then incubated at 60C for 50 minutes and heat inactivated for 10 minutes at 80C. Each reaction was RNAseH (NEB) treated according to manufacturer instructions and cDNA was purified using MinElute Reaction Cleanup Kit (Qiagen). cDNA concentration was determined using Qubit™ ssDNA Assay Kit (Invitrogen™) and then equalized between samples with ddH_2O. qPCR (50 cycles) was performed on a Roche LightCycler480. Reactions were run in triplicates with

PrimeTime Gene Expression Master Mix (IDT) in a total volume of 10µl with standard cycling conditions. hTERT exon1-2 and exon1-3 expression was normalized using hTERT exon3-4 genes and all calculations were performed in Excel. A list of primers is available in Supp. Table 1.

CRISPR/Cas9 targeting

H7 RE2$^{-/-}$, RE3$^{-/-}$ and RE2$^{-/-}$RE3$^{-/-}$ double knockouts polyclonal populations were generated as previously described (#). Briefly H7 cells were transfected with a total of 2 gRNAs targeting the 500bp region for RE2 (TTCCCTTGCCCGCTAGAGGG and CCCCCAAGGGAATGAAAAAG) or RE3 (GTGTCTGGATGGACCAGCAG and GCAATGGTAACTCAGTGACT) cloned in a modified version of vector pX458, a kind gift from Feng Zhang (Addgene plasmid # 48138), and a plasmid DNA donor containing 500bp of upstream and downstream homology sequence for either RE2 or RE3 flanking a hPGK-driven Puromycin resistance gene surrounded by two LoxP sites. Five days following transfection, transfected cells were treated with puromycin (250ng/ml) and surviving clones were subjected to genotyping PCR using primers included in Supp. Table 1. Homozygous targeted clones were expanded and infected using lentivirally encoded Cre-recombinase with a Hygromycin resistance gene. Following infection, cells were treated with hygromycin (100ug/ml) and genotyping PCR was performed to confirm excision of the puromycin cassette by fragment size using primers in Supp. Table 1. H7 hTERT$^{\Delta in/\Delta in}$ ESCs were obtained by delivering a single-stranded 200nt template oligo containing abutting 100nt sequences from hTERT exon-1 and exon-2 and either an RNP complex of a single gRNA targeting hTERT intron-1 (CGGGGGGAACCAGCGACATG), tcrRNA and wild-type Cas9 protein (IDT) or 2 gRNAs targeting hTERT intron-1 (CGCATGTCGCTGGTTCCCCC and CGGGGGGAACCAGCGACATG) cloned into a modified pX458 plasmid described above. Transfected cells were plated at clonal density and individual clones were picked for genotyping approximately one week later. Genotyping was performed by PCR looking for loss of 104bp in PCR amplicon spanning hTERT exons 1-2 (Supp. Table 1). Genomic DNA was extracted using the Quick-DNA Miniprep Kit (Zymo). Genotyping PCR was performed using Failsafe PCR 2x PreMix H (Lucigen) and Taq polymerase (NEB).

Lentiviral delivery

Cre-recombinase and Vp64 Cas9-Activation constructs (19) were purchased in the pLenti backbone (Addgene 73795, 61425, 61426) and were introduced by 4 lentiviral infections at 12hr intervals in presence of 8 µg/ml polybrene (Sigma-Aldrich®) using supernatant from transfected 293T cells. For targeting Vp64-dCas9 to hTERT promoter, two guide RNA sequences were used

in combination (CCAGCTCCGCCTCCTCCGCG and CCAGGACCGCGCTTCCCACG). Vp64 antibiotic resistance genes were replaced with fluorescent protein (mCherry, sfGFP, and tagBFP) genes via several cloning strategies to allow for FACS selection of triple-positive cells containing all Cas9-activation components.

TRAP Assay for telomerase activity

Telomerase Repeat Addition Processivity (TRAP) was performed as described (#). In brief, cells were dissociated and counted on a manual hemocytometer (Fisher Scientific) using Trypan Blue (Corning) to count viable cells. Cells were pelleted and resuspended in CHAPS lysis buffer (Millipore) with Halt Protease+Phosphatase inhibitor (Thermo) and 3μM β-mercaptoethanol at a concentration of $5x10^3$ cells per μl. Lysates were incubated on ice for 30 minutes, vortexed twice during incubation, and then clarified at 12,000g for 20 minutes. Serial dilutions and heat inactivated samples were prepared and 2μl of lysate or dilution was used in each PCR reaction as described in (18). Cycling conditions were as follows: incubate 30 minutes at 30C, boil 5 minutes at 95C, then melt 30 second at 95C, anneal 30 seconds at 59C, extend 1 minute at 72C; 25 cycles were used for ESC samples, 26 cycles for Hela, and 30 cycles for fibroblast and PBMC samples, and in all cases reaction concluded with a final extension for 10 minutes at 72C. Reactions were run on a 10% acrylamide gel (19:1, Fisher Scientific) and imaged on a ChemiDoc MP apparatus (Biorad).

RNA-Capture sequencing for hTERT transcripts

Total RNA was purified with RNAeasy Mini Kit (Qiagen) following manufacturer instructions. Genomic DNA was eliminated by on-column digestion with DNaseI. A total of 25 μg of RNA was reverse-transcribed using Superscript IV Reverse-Transcription kit (Invitrogen) in multiple PCR-tubes using a mix of hTERT specific primers in exon-4, exon-9, exon-12, and exon-16 (Supp. Table 1). Primers were annealed to hTERT RNA at 65C for 5 minutes and then incubated at 0C for 5 minutes before addition of other kit reagents. Reaction was then incubated at 60C for 50 minutes and heat inactivated for 10 minutes at 80C. Each reaction was RNAseH (NEB) treated according to manufacturer instructions and second-strand cDNA was synthesized using Second Strand DNA Synthesis kit (NEB) per manufacturer's instructions. NYU Genome Technology core designed custom probe-library tiling hTERT exons and flanking intragenic sequences using X-Gen probe design software proceeded with Illumina sequencing library preparation of double-stranded cDNA and hybridization and purification of target sequences. Libraries were sequenced using the Illumina MiSeq and data was aligned to hg19 reference genome using Bowtie2 and

alternative splicing analysis performed using TopHat.

Transient Transfection of plasmid DNA and siRNA

Purified plasmid DNA (2-3µg) was introduced to ARPE cells via transient transfection using Lipofectamine 3000 transfection reagent (ThermoFisher) or to H7 ESCs using Genejuice transfection reagent (MilliporeSigma) according to manufacturer's instructions.

For candidate validation experiments, 2-10 pmol of 4-oligo ON-TARGETplus siRNA pools (Horizon, Dharmacon) or non-targeting control pools (Horizon, Dharmacon) were introduced to H7 ESCs and HeLa cells using 4D-Nucleofector™ (Lonza™) electroporation as per manufacturer instructions for each cell line (ESC: CA-137 in P3 solution, HeLa: CN-113 in SE solution). Splice-blocking morpholino (ASO) for hTERT exon-2 5' splice site (AGGACACCTGCGGGGGAAGCG) was ordered from Gene Tools, LLC according to their design recommendations with a 3'-Carboxyfluorescein residue to assess transfection efficiency. ASO was delivered to cells by nucleofection as described above.

hTERT Exon 1-3 splicing minigene assembly by homologous recombination

DNA inserts were PCR amplified with oligos containing the corresponding VEGAS adapters and gel purified while the VEGAS backbone (36) was digested with *Bsa*I and gel purified. ~100 ng of each fragment along with the linearized VEGAS backbone were transformed using the standard lithium acetate method into *Saccharomyces cerevisiae* strain BY4741 (51) and plated onto SC–Ura plates. After 48 hours colonies were replica plated onto SC–Ura plates containing G418. After an additional two days of growth colonies were screened using PCR to verify the presence of each fragment-fragment junction as well as the initial and terminal backbone-fragment junctions. Colonies containing all junctions were grown overnight in liquid SC–Ura media containing G418. Plasmids were extracted from yeast as follows. 1.5 mL of overnight culture was spun down and resuspended in 250 µL P1 buffer with RNAse (Qiagen) and 200 µL of glass beads (Sigma) in an eppendorf tube and shaken for 10 minutes to break the cells. 250 µL of P2 buffer (Qiagen) was added, mixed by inversion, and incubated for 5 minutes at room temperature. 350 µL of P3 buffer (Qiagen) was added and mixed by inversion. This mixture was spun at 10000xg for 10 minutes in a tabletop centrifuge. The supernatant was transferred to a Zyppy miniprep column (Zymo Research) and spun at 10000xg for one minute; the flowthrough was discarded. The column was washed with 200 µL endo wash buffer, spun at 10000xg for one minute, then washed with 400 µL Zyppy wash buffer and spun again for one minute with flow through discarded. The column was spun one more time to remove residual wash buffer. DNA was eluted with 10 µL of elution

buffer. 3 µL of eluted DNA was transformed into *E. coli*. Plasmid DNA recovered from E. coli was digested with AflIII and NotI to release minigene fragment from shuttle vector and clone into pcDNA™5/FRT/TO (Thermo) mammalian expression vector for integration into Hela cells by co-transfection with pOG44-Flpase (Thermo). Hygromycin (150ug/ml) was used to select for cells with integration and Nano-Glo Dual-luciferase assay kit (Promega) was used to confirm expression of both Firefly and Nano-luciferase in clonally isolated cells.

RNAi Luciferase Screen for hTERT alternative splicing factors

4.5 pmol of Ambion® Silencer® Select siRNA pools (ThermoFisher) was spotted in a 96-well plate format and transfection complexes were formed in OptiMEM (Gibco) using Lipofectamine RNAiMAX (Invitrogen™) according to manufacturer's instructions. We then introduced the T-REx™-HeLa cell line with heterozygous integration of two minigene constructs suspended in doxycycline-containing DMEM media and incubated for 48 hours at 37C. Cells were lysed and assayed for luciferase activity using the Nano-Glo Dual-Luciferase Reporter Assay System (Promega) according to the manufacturer's instructions using a EnVision® Multilabel Plate Reader (PerkinElmer). Each plate was assayed in triplicate.

Absolute quantification of hTERT mRNA

Total RNA was purified with RNAeasy Mini Kit (Qiagen) following manufacturer instructions. Genomic DNA was eliminated by on-column digestion with DNaseI. A total of 1 µg of RNA was hybridized for 24 hours with a custom library of multiply-labelled fluorescent oligos per manufacturer's instructions to detect specific hTERT exon-exon junctions to derive and absolute quantification of mature spliced transcripts. Predesigned and validated probes against housekeeping genes, TBP and HPRT, were used for subsequent normalization. Probe sequences are listed in Supp. Table 1. Hybridized RNA:probe mixture was then purified and immobilized on nCounter® chips using nCounter Prep Station (NanoString) and then data was acquired using the nCounter® Digital Analyzer (nCounter® FLEX Analysis System, NanoString). All instruments were run and maintained at the NYU Genome Technology Core. Data was analyzed using nSolver™ software package (v4.0, NanoString).

Immunofluorescence (IF) and microscopy

Cells were plated on 12 mm circular glass coverslips (Fisher Scientific) and analyzed for IF with standard techniques. Briefly, cells were fixed with 4% (v/v) paraformaldehyde in PBS (Santa Cruz Biotechnology, Inc.) for 5 minutes at room temperature. Cells were washed with PBS,

permeabilized with 0.5% (v/v) Triton X for 10 minutes and blocked for 30 minutes with PBS containing 3% goat serum (Sigma-Aldrich®), 1 mg/ml bovine serum albumin (BSA, Sigma-Aldrich®), 0.1% Triton X-100 and 1mM EDTA. Cells were incubated with the same buffer containing primary antibodies for 2 hours at room temperature followed by secondary antibodies incubations for 1 hour at room temperature. Cells were mounted with ProLong Gold Antifade (Thermo Fisher Scientific), imaged on a Nikon Eclipse 55i upright fluorescence microscope at 20X and analyzed with Nikon software. Additional contrast/brightness enhancement and export were performed with Fiji-ImageJ software (52). DNA was counterstained with 5 µg/mL DAPI as needed. A complete list of antibodies used in the study and relative dilutions is available in Suppl. Table 2.

Single-molecule hTERT mRNA FISH

Cells were plated on 12 mm circular glass coverslips (Fisher Scientific) and analyzed for smiRNA-FISH using techniques described by Tsanov et al. (32). In brief, cells were fixed with 4% (v/v) EM-grade paraformaldehyde (Electron Microscopy Sciences) for 20 minutes at room temperature. Cells were washed with RNAse-free PBS, and permeabilized in 70% ethanol for 1 hour at 4C. Cells were rehydrated in RNAse-free 1x SSC buffer containing 15% (v/v) formamide (Sigma-Aldrich®) for 15 minutes and then hybridization solution was applied to coverslips overnight, containing 1x SSC, 15% (v/v) formamide, BSA (2mg/ml, NEB), dextran sulfate (10%, Sigma-Aldrich®), VRC (2mM, NEB), tRNA (0.5mg/ml) and 8pmol of flap-annealed probe oligos for hTERT (IDT) designed using Oligostan (32) software, listed in Supp. Table 1. Flap-annealing of probe oligos was done as in Tsanov et al. (32). After hybridization, cells were washed twice in 1X SSC w/ 15% formamide, and twice with 1x PBS, before DNA was counterstained with 5 µg/mL DAPI. Cells were mounted with ProLong Gold Antifade (Thermo Fisher Scientific), imaged on a Nikon Eclipse Ti2 spinning-disc confocal microscope at 60X and analyzed with Nikon software. Additional contrast/brightness enhancement, quantification of foci and export were performed with Fiji-ImageJ software.

Western blot analysis

Cells were harvested by trypsinization, lysed in RIPA buffer (25 mM Tris-HCl pH 7.6, 150 mM NaCl, 0.1% SDS, 1% NP-40, 1% sodium deoxycholate) at about 10^4 cell/µl. After 2 cycles of water bath sonication at medium settings lysates were incubated at 4˚C on a rotator for additional 30 minutes. Lysates were clarified by spinning 30 minutes at 14800 rpm, 4˚C and supernatant protein concentration was quantified with Enhanced BCA protocol (Thermo Fisher Scientific, Pierce).

Equivalent amounts of proteins were separated on an SDS-page (approximately 30 µg) and transferred to a nitrocellulose membrane. Membranes were blocked in 5% milk in TBST (137 mM NaCl, 2.7 mM KCl, 19 mM Tris Base and 0.1% Tween-20). Incubation with primary antibodies was performed overnight at 4˚C. Membranes were washed and incubated with HRP conjugated secondary antibodies at 1:5000 dilution, developed with Clarity ECL (Biorad) and acquired with a ChemiDoc MP apparatus (Biorad). Antibodies against GAPDH were used as loading control. A full list of antibodies used in the study and relative dilutions is available in Suppl. Table 2.

Table 1: Sequence of oligos used in study.

Primer	Sequence	Use	Reference
hTERT DpnII Reading 1	AATGATACGGCGACCACCGAACACTCTTTCCCTACACGACGCTCTTCCGATCTTTC TTGCTTTGGCCGCTGGCCTGATC	4C Library	This study
hTERT DpnII Reading 2	AATGATACGGCGACCACCGAACACTCTTTCCCTACACGACGCTCTTCCGATCTTTC CGTCTTTGGCCGCTGGCCTGATC	4C Library	
hTERT DpnII Reading 3	AATGATACGGCGACCACCGAACACTCTTTCCCTACACGACGCTCTTCCGATCTTTC GCACTTTGGCCGCTGGCCTGATC	4C Library	
hTERT DpnII Reading 4	AATGATACGGCGACCACCGAACACTCTTTCCCTACACGACGCTCTTCCGATCTTTG GTCCTTTGGCCGCTGGCCTGATC	4C Library	
hTERT DpnII Reading 5	AATGATACGGCGACCACCGAACACTCTTTCCCTACACGACGCTCTTCCGATCTtatt cgCTTTGGCCGCTGGCCTGATC	4C Library	
hTERT DpnII Reading 6	AATGATACGGCGACCACCGAACACTCTTTCCCTACACGACGCTCTTCCGATCTtata gcCTTTGGCCGCTGGCCTGATC	4C Library	
hTERT Csp6I Secondary	CAAGCAGAAGACGGCATACGAAGCTGCGCCTACCAGGTGT	4C Library	
Tert Promoter NcoI F	aaaaaaccatggAAGTCCTCAGCCTTCACGTCCGGCATTCGT	pRF Cloning	This study
Tert Promoter NcoI R	aaaaaaccatgggGGaCAGCGGCAGCACCTCG	pRF Cloning	
RE1 Bsu36I F	aaaaaacctcaggAGTAGGCGGGATCCGGACAG	pRF Cloning	
RE1 Bsu36I R	aaaaaacctgaggCCGAGAAGGAGAAGCATCTGGA	pRF Cloning	
RE2 Bsu36I F	aaaaaacctcaggCTGGCACTGCTGCCTGTGA	pRF Cloning	
RE2 Bsu36I R	aaaaaacctgaggGACCCAGAGGCAGTAAGAGAACG	pRF Cloning	
RE3 BbcCI F	aaaaaacctcagcTCCAGAGATCCCGTGAGAGC	pRF Cloning	
RE3 BbvcI R	aaaaaagctgaggCTGGCTCCCCAGCTTCCTTG	pRF Cloning	
RE4 Bsu36I F	aaaaaacctcaggGGGGCCGAATGACGCTATTT	pRF Cloning	
RE4 Bsu36I R	aaaaaacctgaggCCAGATGAGTTGGCACAGGAAA	pRF Cloning	
RE5 Bsu36I F	aaaaaacctcagggctcgagcCCACCTCCAGCCAAAACAGG	pRF Cloning	
RE5 Bsu36I R	aaaaaacctgagggctcgagcCTGTGGGCTCCTGCAGCTTT	pRF Cloning	
RE6 Bsu36I F	aaaaaacctcagGTCCACGGAGGTCACGTTCAG	pRF Cloning	
RE6 Bsu36I R	aaaaaacctgaggGGCAGCTGGCTTTGCTGAC	pRF Cloning	
RE7 Bsu36I F	aaaaaacctcaggCACAGCACCACGGGCCTATT	pRF Cloning	
RE7 Bsu36I R	aaaaaacctgaggTTGATTTCCTGGCCTTTAAAAATGA	pRF Cloning	
RE8 Bsu36I F	aaaaaacctcaggGCCTTGGACAGCTTGCAGAA	pRF Cloning	
RE8 Bsu36I R	aaaaaacctgaggGCTCAGAATTTGAGGAATTCACACC	pRF Cloning	
TBP F	TGCCCGAAACGCCGAATATAATC	qPCR	Primer Bank
TBP R	GTCTGGACTGTTCTTCACTCTTGG	qPCR	
HPRT1 F	CTTTGCTGACCTGCTGGATT	qPCR	
HPRT1 R	TCCCCTGTTGACTGGTCATT	qPCR	
Col1a1 F	GGACACAGAGGTTTCAGTGGT	qPCR	
Col1a1 R	CACCATCATTTCCACGAGCA	qPCR	
aSMA F	ACTGCCTTGGTGTGTGACAATGG	qPCR	
aSMA R	TGGTGCCAGATCTTTTCCATG	qPCR	
AFP F	TTGGGCTGCTCGCTATG	qPCR	
AFP R	TTTGTAACTGTTGCTGCCTTTG	qPCR	

HNF4a F	CAGGCTCAAGAAATGCTTCC	qPCR	
HNF4a R	GGCTGCTGTCCTCATAGCTT	qPCR	
FGA F	ATGAAACGACTGGAGGTGG	qPCR	
FGA R	TACTTCACGAGCTAAAGCCC	qPCR	
AGT F	ACTTCCAAGGGAAGATGAAGG	qPCR	
AGT R	GAACAGACACTGAGGTGCT	qPCR	
ASGPR F	GAAAGATGAAGTCGCTAGAGT	qPCR	
ASGPR R	AGGCTCCGCAGGTCAGACAC	qPCR	
ALB F	GCCAAGACATATGAAACCAC	qPCR	
ALB R	TTCATCGAACACTTTGGCA	qPCR	
Upf1 F	CTGCAACGGACGTGGAAATAC	qPCR	
Upf1 R	ACAGCCGCAGTTGTAGCAC	qPCR	
Exosc3 F	ACTCTCAGCAGAAGCGGTATG	qPCR	
Exosc3 R	CCTGCACATTTGGTCTGTTTCTT	qPCR	
Mbnl1 F	GGACGAGTAATCGCCTGCTTT	qPCR	
Mbnl1 R	TCTGCTGAATCAAGTTATTGCGT	qPCR	
SON (Exon1-3) F	CAGATTTTTAGGTCTTTCGTGGT	qPCR	Ahn E et al., 2013
SON (Exon1-3) R	TTTTTCTGGAGCCCTCTTTC	qPCR	
TERT Ex4 RT	CCTGACCTCTGCTTCCGACAG	hTERT RT GSP/Capture GSP	This study
TERT Ex9 RT	CTTGTTCTCCATGTCGCCGTAGCAC	Capture GSP	
TERT Ex12 RT	CTGTGACACTTCAGCCGCAAGAC	Capture GSP	
TERT Ex 16 RT	GATGGTCTTGAAGTCTGAGGGC	Capture GSP	
TERT ex1-2 F	CTCCTTCCGCCAGGTGTC	hTERT Junction qPCR	This study
TERT ex1-2 P	CTGCCTGAAGGAGCTGGTGGC	hTERT Junction qPCR	
TERT ex1-2 R	GAAGGCCAGCACGTTCTTC	hTERT Junction qPCR	
TERT e1-3 F	CTCCTTCCGCCAGGGGTTG	hTERT Junction qPCR	
TERT e1-3 P	CGTCGTCGAGCTGCTCAGGTCTTT	hTERT Junction qPCR	
TERT e1-3 R	TTCTTTTGAAACGTGGTCTCC	hTERT Junction qPCR	
TERT e3-4 F	CGGAAGAGTGTCTGGAGCAA	hTERT Junction qPCR	
TERT e3-4 P	ACTCCGCTTCATCCCCAAGC	hTERT Junction qPCR	
TERT e3-4 R	CCCACGACGTAGTCCATGTT	hTERT Junction qPCR	
RE2 F	CCTGAGGACCGGAACCAACTT	Genotype	This study
RE2 R	GGGGAGAGAGAAAGAAGGCTTTCAG	Genotype	
RE3 F	CCGTGAAGTCTAAGGGCAGCTC	Genotype	
RE3 R	GGCGGGCACATTCTTTGTCAACAT	Genotype	
int1 geno F	GTGGCCCAGTGCCTGGTGT	Genotype	
int1 geno R	GGCCTCCCTGACGCTATGGT	Genotype	

dInt1 ssDonor	CCGGCGGCTTTCCGCGCGCTGGTGGCCCAGTGCCTGGTGTGCGTGCCCTGGGAC GCACGGCCGCCCCCCGCCGCCCCCTCCTTCCGCCAGGTGTCCTGCCTGAAGGAGC TGGTGGCCCGAGTGCTGCAGAGGCTGTGCGAGCGCGGCGCGAAGAACGTGCTG GCCTTCGGCTTCGCGCTG	CRISPR ssDNA Donor	This study
Minigene F1 VA1 AflII F	CCCCTTAGGTTGCAAATGCTCCGTCGACGGGATCTGTCCTTCTCTGCCGGCGATC GTcttaagGCGGCGCGAGTTTCAGGC	Minigene Assembly	
Minigene F1 R	CAATTCTGCACTGTACACAGAAAACGGT	Minigene Assembly	
Minigene F2 F	AGACTTCCGGCCATGCAGAC	Minigene Assembly	
Minigene F2 R	AACAGACCCATCCCCCAGGT	Minigene Assembly	
minigene F3 F	GCGGAGCCTTGCTTTGTGATCTAGTGTG	Minigene Assembly	
Minigene F3 R	CCTGGCGACCTCATCCCAGACGTGCACCATCCGGACACTGCACATCCAGCTCACT GAGGGCCTGGCGACCTCATCCCGGACCTGCACCATCTGGTACAAC	Minigene Assembly	
minigene F4 F	CATGGCCATGGCTGTTGTACCAGATG	Minigene Assembly	This study
minigene F4 R	TTGGCCAGGATCTCCTCACGCAGAC	Minigene Assembly	
Minigene FL Firefly F	GCTGTGTTCCGGCCGCAGAGCACCGTCTGCGTGAGGAGATCCTGGCCAAGTTCC TGCACTGGgaggtggcggaACTTcgataGAGGGCAGAGGAAGTCTGCTAACATGCG GTGACGTCGAGGAGAATCCTGGCCCAGAAGACGCCAAAAACATAAAGAAAG	Minigene Assembly	
Minigene FL Firefly NotI VA11 R	ACCACTCGGGCATAGTCCGGAGGTGCTGCGGAGAGTTTACACCTCTTCAAAACTT GCgcggccgcTCTAGAATTACACGGCGATCTTTC	Minigene Assembly	
Minigene dEx2 NanoLuc F	GCTGTGTTCCGGCCGCAGAGCACCGTCTGCGTGAGGAGATCCTGGCCAAGTTCC TGCACTGGCGAGGGCAGAGGAAGTCTGCTAACATGCGGTGACGTCGAGGAGAA TCCTGGCCCAGTCTTCACACTCGAAGATTTCGTTG	Minigene Assembly	
Minigene dEx2 NanoLuc NotI VA11 R	ACCACTCGGGCATAGTCCGGAGGTGCTGCGGAGAGTTTACACCTCTTCAAAACTT GCgcggccgcCCTTACGCCAGAATGCGTTCGC	Minigene Assembly	
HPRT1 Tag	TGTGATGAAGGAGATGGGAGGCCATCACATTGTAGCCCTCTGTGTGCTCAAGGG GGGCTATAAATTCTTTGCTGACCTGCTGGATTACATCAAAGCACTG	Nanostring Probe	
TBP Tag	ACAGTGAATCTTGGTTGTAAACTTGACCTAAAGACCATTGCACTTCGTGCCCGAA ACGCCGAATATAATCCCAAGCGGTTTGCTGCGGTAATCATGAGGA	Nanostring Probe	
TERT_e3-4 Tag	TTTTTCTACCGGAAGAGTGTCTGGAGCAAGTTGCAAAGCATTGGAATCAGACAG CACTTGAAGAGGGTGCAGCTGCGGGAGCTGTCGGAAGCAGAGGTCA	Nanostring Probe	
TERT_e5-6 Tag	TGCTGCGTGTGCGGGCCCAGGACCCGCCGCCTGAGCTGTACTTTGTCAAGGTGG ATGTGACGGGCGCGTACGACACCATCCCCCAGGACAGGCTCACGGA	Nanostring Probe	
TERT_e7-8 Tag	CTCACCTGCAGGAGACCAGCCCGCTGAGGGATGCCGTCGTCATCGAGCAGAGCT CCTCCCTGAATGAGGCCAGCAGTGGCCTCTTCGACGTCTTCCTACG	Nanostring Probe	This study
TERT_e11 Tag	AGTGGTGAACTTCCCTGTAGAAGACGAGGCCCTGGGTGGCACGGCTTTTGTTCA GATGCCGGCCCACGGCCTATTCCCCTGGTGCGGCCTGCTGCTGGAT	Nanostring Probe	
TERT_e14-15 Tag	CTGACACGGCCTCCCTCTGCTACTCCATCCTGAAAGCCAAGAACGCAGGGATGTC GCTGGGGGCCAAGGGCGCCGCCGGCCCTCTGCCCTCCGAGGCCGT	Nanostring Probe	
HPRT1 A Probe	TGAGCACACAGAGGGCTACAATGTGATGGCCTCCCATCTCCTTCATCACACCTCA AGACCTAAGCGACAGCGTGACCTTGTTTCA	Nanostring Probe	
TBP A Probe	GCACGAAGTGCAATGGTCTTTAGGTCAAGTTTACAACCAAGATTCACTGTCACAA TTCTGCGGGTTAGCAGGAAGGTTAGGGAAC	Nanostring Probe	
TERT_e3-4 A Probe	CTGATTCCAATGCTTTGCAACTTGCTCCAGACACTCTTCCGGTAGAAAAACTGTTG AGATTATTGAGCTTCATCATGACCAGAAG	Nanostring Probe	
TERT_e5-6 A Probe	TTTTTCTCATAACACCGCCCGTCACATCCACCTTGACAAAGTACAGCCTTTCGGGT TATATCTATCATTTACTTGACACCCT	Nanostring Probe	
TERT_e7-8 A Probe	CTGCTCGATGACGACGGCATCCCTCAGCGGGCTGGCAAAGACGCCTATCTTCCA GTTTGATCGGGAAACT	Nanostring Probe	

TERT_e11 A Probe	CAAAAGCCGTGCCACCCAGGGCCTCGTCTTCTACAGGGAAGCGAACCTAACTCCTCGCTACATTCCTATTGTTTTC	Nanostring Probe	
TERT_e14-15 A Probe	CCCTGCGTTCTTGGCTTTCAGGATGGAGTAGCAGAGGGAGGCCGTGTCAGCCAATTTGGTTTTACTCCCCTCGATTATGCGGAGT	Nanostring Probe	
HPRT1 B Probe	CGAAAGCCATGACCTCCGATCACTCCAGTGCTTTGATGTAATCCAGCAGGTCAGCAAAGAATTTATAGCCCCCCT	Nanostring Probe	
TBP B Probe	CGAAAGCCATGACCTCCGATCACTCTCCTCATGATTACCGCAGCAAACCGCTTGGGATTATATTCGGCGTTTCGG	Nanostring Probe	
TERT_e3-4 B Probe	CGAAAGCCATGACCTCCGATCACTCCGACAGCTCCCGCAGCTGCACCCTCTTCAAGTGCTGT	Nanostring Probe	
TERT_e5-6 B Probe	CGAAAGCCATGACCTCCGATCACTCTCCGTGAGCCTGTCCTGGGGGATGGTGTCGTACGC	Nanostring Probe	
TERT_e7-8 B Probe	CGAAAGCCATGACCTCCGATCACTCAAGACGTCGAAGAGGCCACTGCTGGCCTCATTCAGGGAGGAGCT	Nanostring Probe	
TERT_e11 B Probe	CGAAAGCCATGACCTCCGATCACTCCGCACCAGGGGAATAGGCCGTGGGCCGGCATCTGAA	Nanostring Probe	
TERT_e14-15 B Probe	CGAAAGCCATGACCTCCGATCACTCAGAGGGCCGGCGGCGCCCTTGGCCCCCAGCGACAT	Nanostring Probe	
TERT 1025	GGAAGTGCTTGGTCTCGGCGTACACCGTTACACTCGGACCTCGTCGACATGCATT	hTERT smiFISH	
TERT 1054	AGCTGCTCCTTGTCGCCTGAGGAGTATTACACTCGGACCTCGTCGACATGCATT	hTERT smiFISH	
TERT 1097	AGTCAGGCTGGGCCTCAGAGAGCTGATTACACTCGGACCTCGTCGACATGCATT	hTERT smiFISH	
TERT 1149	GCATCCAGGGCCTGGAACCCAGAAAGTTACACTCGGACCTCGTCGACATGCATT	hTERT smiFISH	
TERT 1794	CCAATGCTTTGCAACTTGCTCCAGACATTACACTCGGACCTCGTCGACATGCATT	hTERT smiFISH	
TERT 1823	CTGCACCCTCTTCAAGTGCTGTCTGATTACACTCGGACCTCGTCGACATGCATT	hTERT smiFISH	
TERT 1950	CACGACGTAGTCCATGTTCACAATCGGCTTACACTCGGACCTCGTCGACATGCATT	hTERT smiFISH	
TERT 1980	CTCTTTTCTCTGCGGAACGTTCTGGCTTTACACTCGGACCTCGTCGACATGCATT	hTERT smiFISH	
TERT 2239	TTCTGGGGTTTGATGATGCTGGCGATGACTTACACTCGGACCTCGTCGACATGCATT	hTERT smiFISH	
TERT 2324	GTAGAGACGTGGCTCTTGAAGGCCTTGCTTACACTCGGACCTCGTCGACATGCATT	hTERT smiFISH	
TERT 2354	GTCGCATGTACGGCTGGAGGTCTGTCATTACACTCGGACCTCGTCGACATGCATT	hTERT smiFISH	
TERT 2429	CATTCAGGGAGGAGCTCTGCTCGATGATTACACTCGGACCTCGTCGACATGCATT	hTERT smiFISH	This study
TERT 2928	AGCCTTGAAGCCGCGGTTGAAGGTGAGATTACACTCGGACCTCGTCGACATGCATT	hTERT smiFISH	
TERT 2958	CCCAAAGAGTTTGCGACGCATGTTCCTCTTACACTCGGACCTCGTCGACATGCATT	hTERT smiFISH	
TERT 2988	ACAGGCTGTGACACTTCAGCCGCAAGTTACACTCGGACCTCGTCGACATGCATT	hTERT smiFISH	
TERT 3016	CTGGAGGCTGTTCACCTGCAAATCCAGTTACACTCGGACCTCGTCGACATGCATT	hTERT smiFISH	
TERT 3045	AGGAGGATCTTGTAGATGTTGGTGCACACCTTACACTCGGACCTCGTCGACATGCATT	hTERT smiFISH	
TERT 3077	ACATGCGTGAAACCTGTACGCCTGCATTACACTCGGACCTCGTCGACATGCATT	hTERT smiFISH	
TERT 3199	AGCGACATCCCTGCGTTCTTGGCTTTTTACACTCGGACCTCGTCGACATGCATT	hTERT smiFISH	
TERT 3747	ATTCCTATGTGGGGAGTGGAAGCCGGGTTACACTCGGACCTCGTCGACATGCATT	hTERT smiFISH	
TERT 3776	GGGTGAACAATGGCGAATCTGGGGATGGATTACACTCGGACCTCGTCGACATGCATT	hTERT smiFISH	
TERT 3836	CTTCTCAGGGTCTCCACCTGGATGGTTTACACTCGGACCTCGTCGACATGCATT	hTERT smiFISH	
TERT 3866	TCACTCCAAATTCCCAGAGCTCCCAGTTACACTCGGACCTCGTCGACATGCATT	hTERT smiFISH	

TERT 3894	CTCGCCTGTGTACAGGGCACACCTTTTTACACTCGGACCTCGTCGACATGCATT	hTERT smiFISH

Table 3: List of Antibodies used throughout the study.

Primary Antibodies	Host	Company	Catalogue	Dilution
GAPDH (0411)	Mouse	Santa Cruz Biotech.	sc-47724	1:10000 (WB)
SSEA-4 (MC-813-70)	Mouse	R&D Systems	MAB1435	1:500 (IF)
COL1A1 (3G3)	Mouse	Santa Cruz Biotech.	sc-293182	1:500 (IF)
SON	Rabbit	Novus Biologicals	NBP1-88706	1:1000 (WB)
Secondary Antibodies	**Host**	**Company**	**Catalogue**	**Dilution**
Mouse IgG, HRP-linked whole Ab	Sheep	GE Amersham	NA931V	1:5000 (WB)
Rabbit IgG, HRP-linked whole Ab	Donkey	GE Amersham	NA934V	1:5000 (WB)
Alexa Fluor 488 (D-anti-M)	Donkey	Life Technologies	A-21202	1:500 (IF)
Alexa Fluor 568 (D-anti-M)	Donkey	Life Technologies	A-10037	1:500 (IF)

Table 4: List of RNA-binding proteins and splicing factors tested in RNAi screen

AAR2	CWC15	GTF2F1	METTL16	PRMT5	RNF113B	SNU13	TXNL4B
ACIN1	CWC22	GTF2F2	METTL3	PRMT7	Rnf219	SNUPN	U2AF1
AFF2	CWC25	HABP4	MFAP1	PRPF18	RNPC3	SNW1	U2AF1L4
AHNAK	CWC27	HMX2	MPHOSPH10	PRPF19	RNPS1	SON	U2AF2
AHNAK2	CWF19L1	HNRNPA0	MYOD1	PRPF3	RP9	SREK1	U2SURP
AKAP17A	CWF19L2	HNRNPA1	NCBP1	PRPF31	RPS13	SREK1IP1	UBL5
AKAP8L	DAZAP1	HNRNPA1L2	NCBP2	PRPF38A	RPS26	SRPK1	UPF3B
AKT2	DBR1	HNRNPA2B1	NOL3	PRPF38B	RRAGC	SRPK2	USB1
ALYREF	DCPS	HNRNPA3	NONO	PRPF39	RRP1B	SRPK3	USP39
AQR	DDX1	HNRNPC	NOVA1	PRPF4	RSRC1	SRRM1	USP4
ARL6IP4	DDX17	HNRNPD	NOVA2	PRPF40A	RTCB	SRRM2	USP49
BCAS2	DDX20	HNRNPF	Npm1	PRPF40B	SAP18	SRRM4	WBP11
BRDT	DDX23	HNRNPH1	NSRP1	PRPF4B	SART1	SRRT	WBP4
BUD13	DDX39A	HNRNPH2	NUDT21	PRPF6	SART3	SRSF1	WDR33
BUD31	DDX39B	HNRNPH3	NUP98	PRPF8	SCAF1	SRSF10	WDR77
C1QBP	DDX41	HNRNPK	PABPC1	PRX	SCAF11	SRSF11	WDR83
C2orf49	DDX42	HNRNPL	PABPN1	PSIP1	SCAF8	SRSF12	WT1
C9orf78	DDX46	HNRNPLL	PAPOLA	PTBP1	SCNM1	SRSF2	WTAP
CACTIN	DDX47	HNRNPM	PCBP1	PTBP2	SETX	SRSF3	XAB2
CASC3	DDX5	HNRNPR	PCBP2	PTBP3	SF1	SRSF4	YBX1
CCAR1	DHX15	HNRNPU	Pcbp4	PUF60	SF3A1	SRSF5	YTHDC1
CCAR2	DHX16	HNRNPUL1	PCF11	QKI	SF3A2	SRSF6	ZBTB7A

CD2BP2	DHX35	HSPA1A	PDCD7	RALY	SF3A3	SRSF7	ZBTB8OS
CDC40	DHX38	HSPA8	PHF5A	RBFOX1	SF3B1	SRSF8	ZC3H10
CDC5L	DHX40	HTATSF1	PIK3R1	RBFOX2	SF3B2	SRSF9	ZC3H13
CDK12	DHX8	IK	PLRG1	RBFOX3	SF3B3	STH	ZCCHC8
CDK13	DHX9	ISY1	PNN	RBM10	SF3B4	STRAP	ZCRB1
CELF1	DNAJC8	IVNS1ABP	POLR2A	RBM11	SF3B5	SUGP1	ZMAT2
CELF2	DYRK1A	IWS1	POLR2B	RBM15	SF3B6	SUGP2	ZMAT5
CELF3	ECD	JMJD6	POLR2C	RBM15B	SFPQ	SUPT6H	ZNF326
CELF4	EFTUD2	KDM1A	POLR2D	RBM17	SFSWAP	SYF2	ZNF638
CELF5	EIF4A3	KHDRBS1	POLR2E	RBM19	SLC39A5	SYMPK	ZNF830
CELF6	ELAVL1	KHDRBS2	POLR2F	RBM20	SLU7	SYNCRIP	ZPR1
CHERP	ELAVL2	KHDRBS3	POLR2G	RBM22	SMNDC1	TAF15	ZRANB2
CIR1	ERN1	KHSRP	POLR2H	RBM24	SMU1	TARDBP	ZRSR2
CIRBP	ESRP1	LGALS3	POLR2I	RBM25	SNIP1	TFIP11	RBM14
CLASRP	ESRP2	Lmntd2	POLR2J	RBM28	SNRNP200	TGS1	FUBP1
CLK1	FAM172A	LSM1	POLR2K	RBM3	SNRNP25	THOC1	CCDC130
CLK2	FAM98B	LSM10	POLR2L	RBM38	SNRNP27	THOC2	EWSR1
CLK3	FASTK	LSM2	PPARGC1A	RBM39	SNRNP35	THOC3	USP43
CLK4	FIP1L1	LSM3	PPIE	RBM4	SNRNP40	THOC5	PCBP3
CLNS1A	FMR1	LSM4	PPIG	RBM41	SNRNP48	THOC6	CCDC94
CLP1	FRG1	LSM5	PPIH	RBM42	SNRNP70	THOC7	RAVER2
COIL	FUS	LSM6	PPIL1	RBM4B	SNRPA	THRAP3	IGF2BP2
CPSF1	FXR1	LSM7	PPIL3	RBM5	SNRPA1	TIA1	RBPMS2
CPSF2	FXR2	LSM8	PPP1R8	RBM7	SNRPB	TMBIM6	RAVER1
CPSF3	GCFC2	LUC7L	PPP1R9B	RBM8A	SNRPB2	TRA2A	USP31
CPSF4	GEMIN2	LUC7L2	PPP2CA	RBMX	SNRPC	TRA2B	NCL
CPSF7	GEMIN4	LUC7L3	PPP2R1A	RBMX2	SNRPD1	TRPT1	IGF2BP3
CRNKL1	GEMIN5	MAGOH	PPP4R2	RBMXL1	SNRPD2	TSEN15	FUBP3
CSTF1	GEMIN6	MAGOHB	PPWD1	RBMXL2	SNRPD3	TSEN2	IGF2BP1
CSTF2	GEMIN7	MBNL1	PQBP1	RBMXL3	SNRPE	TSEN34	RBPMS
CSTF2T	GEMIN8	MBNL2	PRCC	RBMY1F	SNRPF	TSEN54	PSPC1
CSTF3	GPATCH1	MBNL3	PRDX6	REST	SNRPG	TTF2	METTL25
CTNNBL1	GPKOW	METTL14	PRKRIP1	RNF113A	SNRPN	TXNL4A	FTO

References:

1. Feng J, Funk WD, Wang SS, Weinrich SL, Avilion AA, Chiu CP, et al. The RNA component of human telomerase. Science. 1995;269(5228):1236-41.
2. Venteicher AS, Meng Z, Mason PJ, Veenstra TD, Artandi SE. Identification of ATPases pontin and reptin as telomerase components essential for holoenzyme assembly. Cell. 2008;132(6):945-57.
3. Meyerson M, Counter CM, Eaton EN, Ellisen LW, Steiner P, Caddle SD, et al. hEST2, the putative human telomerase catalytic subunit gene, is up-regulated in tumor cells and during immortalization. Cell. 1997;90(4):785-95.
4. Wright WE, Piatyszek MA, Rainey WE, Byrd W, Shay JW. Telomerase activity in human germline and embryonic tissues and cells. Dev Genet. 1996;18(2):173-9.
5. Shay JW, Wright WE. Role of telomeres and telomerase in cancer. Semin Cancer Biol. 2011;21(6):349-53.
6. Takahashi K, Tanabe K, Ohnuki M, Narita M, Ichisaka T, Tomoda K, et al. Induction of pluripotent stem cells from adult human fibroblasts by defined factors. Cell. 2007;131(5):861-72.
7. Batista LF, Pech MF, Zhong FL, Nguyen HN, Xie KT, Zaug AJ, et al. Telomere shortening and loss of self-renewal in dyskeratosis congenita induced pluripotent stem cells. Nature. 2011;474(7351):399-402.
8. Kim NW, Piatyszek MA, Prowse KR, Harley CB, West MD, Ho PL, et al. Specific association of human telomerase activity with immortal cells and cancer. Science. 1994;266(5193):2011-5.
9. Horn S, Figl A, Rachakonda PS, Fischer C, Sucker A, Gast A, et al. TERT promoter mutations in familial and sporadic melanoma. Science. 2013;339(6122):959-61.
10. Huang FW, Hodis E, Xu MJ, Kryukov GV, Chin L, Garraway LA. Highly recurrent TERT promoter mutations in human melanoma. Science. 2013;339(6122):957-9.
11. Chiba K, Johnson JZ, Vogan JM, Wagner T, Boyle JM, Hockemeyer D. Cancer-associated TERT promoter mutations abrogate telomerase silencing. Elife. 2015;4.
12. Wu KJ, Grandori C, Amacker M, Simon-Vermot N, Polack A, Lingner J, et al. Direct activation of TERT transcription by c-MYC. Nat Genet. 1999;21(2):220-4.
13. van de Werken HJ, de Vree PJ, Splinter E, Holwerda SJ, Klous P, de Wit E, et al. 4C technology: protocols and data analysis. Methods Enzymol. 2012;513:89-112.
14. Raviram R, Rocha PP, Muller CL, Miraldi ER, Badri S, Fu Y, et al. 4C-ker: A Method to Reproducibly Identify Genome-Wide Interactions Captured by 4C-Seq Experiments. PLoS Comput Biol. 2016;12(3):e1004780.
15. Buenrostro JD, Wu B, Chang HY, Greenleaf WJ. ATAC-seq: A Method for Assaying Chromatin Accessibility Genome-Wide. Curr Protoc Mol Biol. 2015;109:21 9 1-9.
16. Akincilar SC, Khattar E, Boon PL, Unal B, Fullwood MJ, Tergaonkar V. Long-Range Chromatin Interactions Drive Mutant TERT Promoter Activation. Cancer Discov. 2016;6(11):1276-91.
17. Davis CA, Hitz BC, Sloan CA, Chan ET, Davidson JM, Gabdank I, et al. The Encyclopedia of DNA elements (ENCODE): data portal update. Nucleic Acids Res. 2018;46(D1):D794-D801.
18. Mender I, Shay JW. Telomerase Repeated Amplification Protocol (TRAP). Bio Protoc. 2015;5(22).
19. Konermann S, Brigham MD, Trevino AE, Joung J, Abudayyeh OO, Barcena C, et al. Genome-scale transcriptional activation by an engineered CRISPR-Cas9 complex. Nature. 2015;517(7536):583-8.
20. Toh CX, Chan JW, Chong ZS, Wang HF, Guo HC, Satapathy S, et al. RNAi Reveals Phase-Specific Global Regulators of Human Somatic Cell Reprogramming. Cell Rep. 2016;15(12):2597-607.

21. Das S, Jena S, Levasseur DN. Alternative splicing produces Nanog protein variants with different capacities for self-renewal and pluripotency in embryonic stem cells. J Biol Chem. 2011;286(49):42690-703.
22. Gabut M, Samavarchi-Tehrani P, Wang X, Slobodeniuc V, O'Hanlon D, Sung HK, et al. An alternative splicing switch regulates embryonic stem cell pluripotency and reprogramming. Cell. 2011;147(1):132-46.
23. Han H, Irimia M, Ross PJ, Sung HK, Alipanahi B, David L, et al. MBNL proteins repress ES-cell-specific alternative splicing and reprogramming. Nature. 2013;498(7453):241-5.
24. Venables JP, Lapasset L, Gadea G, Fort P, Klinck R, Irimia M, et al. MBNL1 and RBFOX2 cooperate to establish a splicing programme involved in pluripotent stem cell differentiation. Nat Commun. 2013;4:2480.
25. Yamazaki T, Liu L, Lazarev D, Al-Zain A, Fomin V, Yeung PL, et al. TCF3 alternative splicing controlled by hnRNP H/F regulates E-cadherin expression and hESC pluripotency. Genes Dev. 2018;32(17-18):1161-74.
26. Hrdlickova R, Nehyba J, Bose HR, Jr. Alternatively spliced telomerase reverse transcriptase variants lacking telomerase activity stimulate cell proliferation. Mol Cell Biol. 2012;32(21):4283-96.
27. Wong MS, Wright WE, Shay JW. Alternative splicing regulation of telomerase: a new paradigm? Trends Genet. 2014;30(10):430-8.
28. Yi X, Shay JW, Wright WE. Quantitation of telomerase components and hTERT mRNA splicing patterns in immortal human cells. Nucleic Acids Res. 2001;29(23):4818-25.
29. Withers JB, Ashvetiya T, Beemon KL. Exclusion of exon 2 is a common mRNA splice variant of primate telomerase reverse transcriptases. PLoS One. 2012;7(10):e48016.
30. Hug N, Longman D, Caceres JF. Mechanism and regulation of the nonsense-mediated decay pathway. Nucleic Acids Res. 2016;44(4):1483-95.
31. Bodnar AG, Ouellette M, Frolkis M, Holt SE, Chiu CP, Morin GB, et al. Extension of life-span by introduction of telomerase into normal human cells. Science. 1998;279(5349):349-52.
32. Tsanov N, Samacoits A, Chouaib R, Traboulsi AM, Gostan T, Weber C, et al. smiFISH and FISH-quant - a flexible single RNA detection approach with super-resolution capability. Nucleic Acids Res. 2016;44(22):e165.
33. Mallanna SK, Duncan SA. Differentiation of hepatocytes from pluripotent stem cells. Curr Protoc Stem Cell Biol. 2013;26:1G 4 1-G 4 13.
34. Barbieri I, Tzelepis K, Pandolfini L, Shi J, Millan-Zambrano G, Robson SC, et al. Promoter-bound METTL3 maintains myeloid leukaemia by m(6)A-dependent translation control. Nature. 2017;552(7683):126-31.
35. Yue Y, Liu J, He C. RNA N6-methyladenosine methylation in post-transcriptional gene expression regulation. Genes Dev. 2015;29(13):1343-55.
36. Mitchell LA, Chuang J, Agmon N, Khunsriraksakul C, Phillips NA, Cai Y, et al. Versatile genetic assembly system (VEGAS) to assemble pathways for expression in S. cerevisiae. Nucleic Acids Res. 2015;43(13):6620-30.
37. Huang da W, Sherman BT, Lempicki RA. Systematic and integrative analysis of large gene lists using DAVID bioinformatics resources. Nat Protoc. 2009;4(1):44-57.
38. Yamazaki T, Souquere S, Chujo T, Kobelke S, Chong YS, Fox AH, et al. Functional Domains of NEAT1 Architectural lncRNA Induce Paraspeckle Assembly through Phase Separation. Mol Cell. 2018;70(6):1038-53 e7.
39. Lu X, Goke J, Sachs F, Jacques PE, Liang H, Feng B, et al. SON connects the splicing-regulatory network with pluripotency in human embryonic stem cells. Nat Cell Biol. 2013;15(10):1141-52.
40. Sharma A, Markey M, Torres-Munoz K, Varia S, Kadakia M, Bubulya A, et al. Son maintains accurate splicing for a subset of human pre-mRNAs. J Cell Sci. 2011;124(Pt 24):4286-98.

41. Kim JH, Shinde DN, Reijnders MRF, Hauser NS, Belmonte RL, Wilson GR, et al. De Novo Mutations in SON Disrupt RNA Splicing of Genes Essential for Brain Development and Metabolism, Causing an Intellectual-Disability Syndrome. Am J Hum Genet. 2016;99(3):711-9.
42. Niewisch MR, Savage SA. An update on the biology and management of dyskeratosis congenita and related telomere biology disorders. Expert Rev Hematol. 2019;12(12):1037-52.
43. Tan TC, Rahman R, Jaber-Hijazi F, Felix DA, Chen C, Louis EJ, et al. Telomere maintenance and telomerase activity are differentially regulated in asexual and sexual worms. Proc Natl Acad Sci U S A. 2012;109(11):4209-14.
44. Rousseau P, Khondaker S, Zhu S, Lauzon C, Mai S, Autexier C. An intact putative mouse telomerase essential N-terminal domain is necessary for proper telomere maintenance. Biol Cell. 2016;108(4):96-112.
45. Moon DH, Segal M, Boyraz B, Guinan E, Hofmann I, Cahan P, et al. Poly(A)-specific ribonuclease (PARN) mediates 3'-end maturation of the telomerase RNA component. Nat Genet. 2015;47(12):1482-8.
46. Alter BP, Giri N, Savage SA, Rosenberg PS. Cancer in the National Cancer Institute inherited bone marrow failure syndrome cohort after fifteen years of follow-up. Haematologica. 2018;103(1):30-9.
47. Miele A, Dekker J. Mapping cis- and trans- chromatin interaction networks using chromosome conformation capture (3C). Methods Mol Biol. 2009;464:105-21.
48. Buenrostro JD, Giresi PG, Zaba LC, Chang HY, Greenleaf WJ. Transposition of native chromatin for fast and sensitive epigenomic profiling of open chromatin, DNA-binding proteins and nucleosome position. Nat Methods. 2013;10(12):1213-8.
49. Corces MR, Trevino AE, Hamilton EG, Greenside PG, Sinnott-Armstrong NA, Vesuna S, et al. An improved ATAC-seq protocol reduces background and enables interrogation of frozen tissues. Nat Methods. 2017;14(10):959-62.
50. Kondrashov N, Pusic A, Stumpf CR, Shimizu K, Hsieh AC, Ishijima J, et al. Ribosome-mediated specificity in Hox mRNA translation and vertebrate tissue patterning. Cell. 2011;145(3):383-97.
51. Brachmann CB, Davies A, Cost GJ, Caputo E, Li J, Hieter P, et al. Designer deletion strains derived from Saccharomyces cerevisiae S288C: a useful set of strains and plasmids for PCR-mediated gene disruption and other applications. Yeast. 1998;14(2):115-32.
52. Schindelin J, Arganda-Carreras I, Frise E, Kaynig V, Longair M, Pietzsch T, et al. Fiji: an open-source platform for biological-image analysis. Nat Methods. 2012;9(7):676-82.